

Article

Optimal Reactive Power Dispatch Using a Chaotic Turbulent Flow of Water-Based Optimization Algorithm

Ahmed M. Abd-El Wahab ^{1,*}, Salah Kamel ^{1,*} , Mohamed H. Hassan ¹ , Mohamed I. Mosaad ^{2,*} 
and Tarek A. AbdulFattah ³

¹ Department of Electrical Engineering, Faculty of Engineering, Aswan University, Aswan 81542, Egypt; eng8080_ahmed@yahoo.com (A.M.A.-E.W.); mohamed.hosny@moere.gov.eg (M.H.H.)

² Electrical & Electronics Engineering Technology Department, Royal Commission Yanbu Colleges & Institutes, Yanbu 46452, Saudi Arabia

³ Department of Engineering Physics and Mathematics, Faculty of Engineering, Zagazig University, Zagazig 44519, Egypt; taabdufatah@gmail.com

* Correspondence: skamel@aswu.edu.eg (S.K.); habibm@rcyci.edu.sa (M.I.M.)

Abstract: In this study, an optimization algorithm called chaotic turbulent flow of water-based optimization (CTFWO) algorithm is proposed to find the optimal solution for the optimal reactive power dispatch (ORPD) problem. The ORPD is formulated as a complicated, mixed-integer nonlinear optimization problem, comprising control variables which are discrete and continuous. The CTFWO algorithm is used to minimize voltage deviation (VD) and real power loss (P_{loss}) for IEEE 30-bus and IEEE 57-bus power systems. These goals can be achieved by obtaining the optimized voltage values of the generator, the transformer tap changing positions, and the reactive compensation. In order to evaluate the ability of the proposed algorithm to obtain ORPD problem solutions, the results of the proposed CTFWO algorithm are compared with different algorithms, including artificial ecosystem-based optimization (AEO), the equilibrium optimizer (EO), the gradient-based optimizer (GBO), and the original turbulent flow of water-based optimization (TFWO) algorithm. These are also compared with the results of the evaluated performance of various methods that are used in many recent papers. The experimental results show that the proposed CTFWO algorithm has superior performance, and is competitive with many state-of-the-art algorithms outlined in some of the recent studies in terms of solution accuracy, convergence rate, and stability.

Keywords: optimal reactive power dispatch; chaotic maps; turbulent flow of water-based optimization; real power loss; voltage deviation



Citation: Abd-El Wahab, A.M.; Kamel, S.; Hassan, M.H.; Mosaad, M.I.; AbdulFattah, T.A. Optimal Reactive Power Dispatch Using a Chaotic Turbulent Flow of Water-Based Optimization Algorithm. *Mathematics* **2022**, *10*, 346. <https://doi.org/10.3390/math10030346>

Academic Editors: Adrian Deaconu, Petru Adrian Coffas and Daniel Tudor Coffas

Received: 28 December 2021

Accepted: 19 January 2022

Published: 24 January 2022

Publisher's Note: MDPI stays neutral with regard to jurisdictional claims in published maps and institutional affiliations.



Copyright: © 2022 by the authors. Licensee MDPI, Basel, Switzerland. This article is an open access article distributed under the terms and conditions of the Creative Commons Attribution (CC BY) license (<https://creativecommons.org/licenses/by/4.0/>).

1. Introduction

The optimal reactive power dispatch (ORPD) problem plays a very important role in the optimal operation of electric power systems. It is a subclass of the optimal power flow (OPF) problem [1]. The power system must be operating with high reliability, and finding a safe way to achieve this should obtain the optimal operating state and the control variable values (such as the generator voltage ratings, the tap ratios for the tap setting transformers, and the reactive power of the shunt capacitors/reactors) [2]. There are three main objectives of ORPD, which include reducing and minimizing the active power losses, the voltage deviation values, and the stability index. Researchers have studied several problems related to the power systems, including the security assessment of online power systems [3], a two-stage active and reactive power coordinated optimal dispatch for an active distribution network, considering load flexibility [4], the early detection and prevention of blackouts in power interconnections [5], OPF [6], and economic emissions dispatch [7].

Recently, different optimization methods have been studied to solve the ORPD problem; various optimization methodologies are recommended, such as deterministic and metaheuristic algorithms [8]. These algorithms include original, modified deterministic,

original, modified metaheuristic, and crossbreed heuristic algorithms [9]. Deterministic algorithms are the earliest methods, and these involve minimizing real power losses using the interior point method, Newton method, quadratic programming method, and an ANN-based memory model [10–13].

Metaheuristic algorithms, such as the genetic algorithm (GA) [14–19], which mimics the rule of natural selection or hereditaries, relate to the terms of genetics and mutation selection. Another algorithm, SARCGA, considers the updating of RCGA to be self-adaptive [14]. Another technique is linear programming with the genetic algorithm [15]. For handling the ORPD problem when considering power loss minimization, the SGA algorithm was introduced in [16]. The hybrid loop-genetic-based algorithm [17] and the adaptive genetic algorithm (AGA) [18] are also used to solve the ORPD problem. Additionally, the enhancement of a new evolutionary GA through the addition of a specific mechanism is achieved in [19]. The particle swarm optimizer (PSO) is a different technique for optimization that is no less famous than the GA. Additionally, it has been used with other algorithms to create new hybrid techniques, such as the imperialist competitive algorithm (HPSO-ICA) [20], aging leader and challengers (ALC-PSO) [21], the original PSO for OPF [22], PSO for ORPD [23], HPSO-TS [24], PSO-GT [25], improved pseudo-gradient (PSO-IPG) [26], and a lot of variant methods, including CLPSO [27] and hybrid particle swarm optimization and differential evolution (HPSO) [28]. Moreover, the differential evolution (DE) algorithm is used to solve the ORPD problem [29], which is also achieved in combination with other algorithms, such as DE-AS [30], quasi-oppositional DE (QODE) [31], CAB-DE [32], and MTLA-DDE [33].

Not only are there the above methods, but there are a lot of other methods that are used to solve the ORPD problem through various systems and techniques, with a single objective or multiple objectives. These methods are improved, such as the gravitational search algorithm (GSA) [34–36], the exchange market optimization algorithm (EMOA) [37], the artificial bee colony (ABC) with firefly algorithm (ABC-FF) [38], the ant lion optimizer (ALO) [39], moth flame optimization (MFO) [40], the cuckoo search optimization algorithm (CSOA) [41], the differential search algorithm (DSA) [42], the multi-objective grey wolf algorithm (MOGWA) [43], improved colliding bodies optimization (ICBO) [44], the Jaya algorithm (JA) [45], the whale optimization algorithm (WOA) [46], ant colony optimization (ACO) [47], the harmony search algorithm (HAS) [48], Gaussian bare-bones teaching–learning-based optimization (GBTLBO) [49], the hybrid Nelder–Mead simplex-based firefly algorithm (HFA-NMS) [50], the Gaussian bare-bones water cycle algorithm (GBBWCA) [51], the gray wolf optimizer (GWO) [52], the cuckoo search algorithm (CSA) [53], the chaotic krill herd algorithm (CKHA) [54], ABC [55], quasi-oppositional teaching–learning-based optimization (QOTLBO) and TLBO [2], the Rao-3 algorithm [56], and the improved Cuckoo search algorithm (ICSA) [57]. Among these methods, there are methods that have improved upon the original methods to find more promising solutions than those of the original methods for the ORPD problem.

This paper suggests a new modification of the TFWO algorithm based on the chaotic maps, which is named the chaotic turbulent flow of water-based optimization (CTFWO) algorithm, to solve the optimum reactive power dispatch problem. The conventional TFWO algorithm was developed by Ghasemi, Mojtaba, et al. in 2020 [58]. The original TFWO algorithm was used to solve many problems, such as the estimation of the parameters of photovoltaic (PV) models [59,60], the maximum power point tracking (MPPT) of photovoltaic systems in partial shading conditions [61], economic load dispatch [62], the optimal settings of back-to-back voltage source converters (BTB-VSC) in an interconnected power system [63], and the optimal allocation of shunt compensators in distribution systems [64]; therefore, we selected it for modification to improve the global search ability and to increase the local search capability and the convergence precision. Meanwhile, we tested it to try and achieve the best results for different single-objective functions, including the minimization of power losses and voltage deviation in two tested power systems. The main contributions of this article are summarized as:

1. Applying four different algorithms as search algorithms, including artificial ecosystem-based optimization (AEO), the equilibrium optimizer (EO), the gradient-based optimizer (GBO), and turbulent flow of water-based optimization (TFWO), on IEEE 30-bus and IEEE 57-bus power systems to solve ORPD problem.
2. The TFWO algorithm gives the best results for different single-objective functions, namely, the minimization of power losses and voltage deviation in both tested power systems.
3. Proposing a new chaotic TFWO algorithm (CTFWO), which based on applying the chaotic approach to improve the performance of the original TFWO
4. The proposed CTFWO algorithm solves the ORPD problem and gives better results than all other compared algorithms on the tested power systems, the 30-bus and the 57-bus systems, for all studied cases.

The rest of the paper is organized as follows:

The ORPD problem is formulated in Section 2. In Section 3.1 the conventional TFWO algorithm is described and in Section 3.2 the proposed CTFWO algorithm is explained. In Section 4, the main achieved results and discussion are given. In Section 5, the conclusion drawn from this research is illustrated.

2. Materials and Methods

The ORPD has three main objectives: first, minimize and reduce the active power losses (P_{loss}); second, reduce the voltage deviation (VD), which is the difference between load voltage (which changes continually) and the reference voltage (with a value of 1.0 pu); finally, minimize the stability index (L-index), which takes values from 0 to 1, with 0 meaning that the system is stable and 1 meaning that there is a system disturbance.

2.1. Objective Functions

The two key objectives of this paper are as follows:

2.1.1. Minimization of the Active Power Loss

When operating any power systems, we can consider that the total active power loss is the main objective of the ORPD:

$$f_1 = \min(P_{loss}) = \min \left[\sum_{k=1}^{N_{TL}} G_k \left(V_i^2 + V_j^2 - 2V_iV_j \cos \alpha_{ij} \right) \right] \tag{1}$$

where:

P_{loss} is the active power loss.

G_k is the conductance of the k th branch connected between the i th and the j th bus.

α_{ij} is the admittance angle of the transmission line connected between the i th and the j th bus.

N_{TL} is the number of transmission lines (branches).

V_i and V_j are the voltage magnitudes of the i th and the j th bus, respectively.

2.1.2. Improvement of the Voltage Profile

The difference between the voltage magnitude at each load bus and what the specified reference value of the voltage ought to be is outlined in the following equation:

$$f_2 = \min \left(\sum_{i=1}^{N_L} |V_{li} - V_{li}^{SP}| \right) \tag{2}$$

where:

V_{li} is the voltage at the i th load bus.

V_{li}^{SP} is the desired voltage at the i th load bus, which is usually set to (1.0 p.u).

N_L is the number of load buses [2,65,66].

2.2. System Constraints

2.2.1. Equality Constraint

This constraint ensures that there is load balance (i.e., the generation of real and reactive power is balanced against consuming):

$$P_i - V_i \sum_{j=1}^{N_B} V_j [G_{ij} \cos(\theta_i - \theta_j) + B_{ij} \sin(\theta_i - \theta_j)] = 0 \tag{3}$$

For $i = 1, \dots, N_B$

$$Q_i - V_i \sum_{j=1}^{N_B} V_j [G_{ij} \sin(\theta_i - \theta_j) - B_{ij} \cos(\theta_i - \theta_j)] = 0 \tag{4}$$

For $i = 1, \dots, N_B$

where:

$P_i = (P_{Gi} - P_{Di})$ and $Q_i = (Q_{Gi} - Q_{Di})$ represent the real and reactive power injection at bus i .

P_{Gi} and Q_{Gi} are the active and reactive power generation of the i th bus.

P_{Di} and Q_{Di} are the active and reactive load demand of the i th bus.

G_{ij} is the real part of the bus admittance matrix of the (i, j) th entry.

B_{ij} is the imaginary part of the bus admittance matrix of the (i, j) th entry.

N_B is numbers of buses.

2.2.2. Inequality Constraints

The inequality constraints should be within limited values, as follow:

$$V_{Gi}^{min} \leq V_{Gi} \leq V_{Gi}^{max} \tag{5}$$

For $i = 1, \dots, N_G$

$$Q_{Ci}^{min} \leq Q_{Ci} \leq Q_{Ci}^{max} \tag{6}$$

For $i = 1, \dots, N_C$

$$T_i^{min} \leq T_i \leq T_i^{max} \tag{7}$$

For $i = 1, \dots, N_T$

where:

V_{Gi}^{min} and V_{Gi}^{max} are the minimum and maximum generator voltage values of the i th bus, respectively.

Q_{Ci}^{min} and Q_{Ci}^{max} are the minimum and maximum values of the reactive power injection of the i th shunt compensator, respectively.

T_i^{min} and T_i^{max} are the minimum and maximum tap setting values of the i th transmission line, respectively.

N_C , N_G , and N_T are the numbers of shunt compensators, generators, and tap changing transformers, respectively.

The inequality constraints on the dependent variable are given by:

$$V_{Li}^{min} \leq V_{Li} \leq V_{Li}^{max} \tag{8}$$

For $i = 1, \dots, N_L$

$$Q_{Gi}^{min} \leq Q_{Gi} \leq Q_{Gi}^{max} \tag{9}$$

For $i = 1, \dots, N_G$.

$$S_{Li} \leq S_{Li}^{max} \tag{10}$$

For $i = 1, \dots, \dots, N_L$
 where:
 V_{Li}^{min} and V_{Li}^{max} are the minimum and maximum voltages of the i th load bus, respectively.
 Q_{Gi}^{min} and Q_{Gi}^{max} are the minimum and maximum reactive power generation values of the i th generator bus, respectively.
 S_{Li}^{max} is the maximum apparent power flow through the i th line [2,65,66].

3. Methodology

3.1. The Conventional TFWO

In this subsection, we briefly explain the concept of the original turbulent flow of water-based optimization (TFWO) algorithm. It is inspired by the whirlpools created in the turbulent flow of water. The whirlpool (Whj) is a random behavior of nature that happens in seas, rivers, and oceans. Its rotation and flow are affected by the force of gravity. The center of the whirlpool (Whj) functions as a sucking hole that attracts the objects and particles nearby towards its middle via internal forces. Though the centripetal force attracts the moving objects towards the whirlpool, the centrifugal force takes the object away from the corresponding center. The effects of the Whj on the object's particles are displayed in Figure 1. As can be seen from Figure 2, the objects (X) move with their special angle (δ) around the Whj's center. Therefore, this angle at each moment is changing as follows:

$$\delta_i^{new} = \delta_i + rand_1 \times rand_2 \times \pi \tag{11}$$

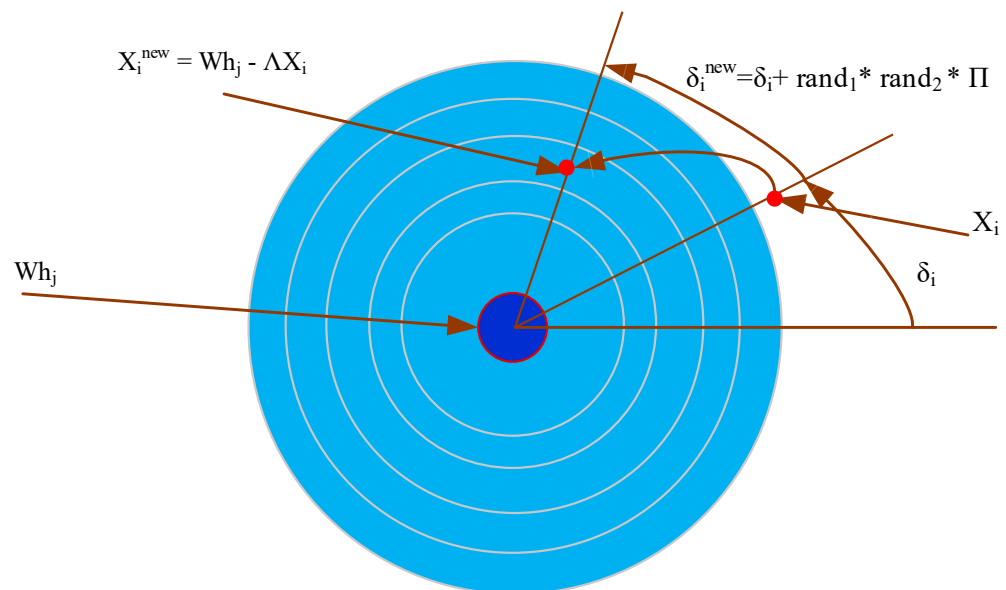


Figure 1. The proposed model of a whirlpool for the TFWO algorithm.

3.2. The Proposed CTFWO

The proposed CTFWO technique is the combination of the conventional TFWO algorithm with chaotic maps. Chaotic systems are deterministic systems that present unpredictable conduct, whose action is complex and similar to randomness [67]. In [67], a chaos-based exploration rate was proposed to enhance the performance of three well-known optimization algorithms. Based on this proposed, the real random numbers ($rand_1, rand_2$) in Equation (11) are replaced by a chaotic number. Figure 2 displays the flow chart of the proposed CTFWO algorithm.

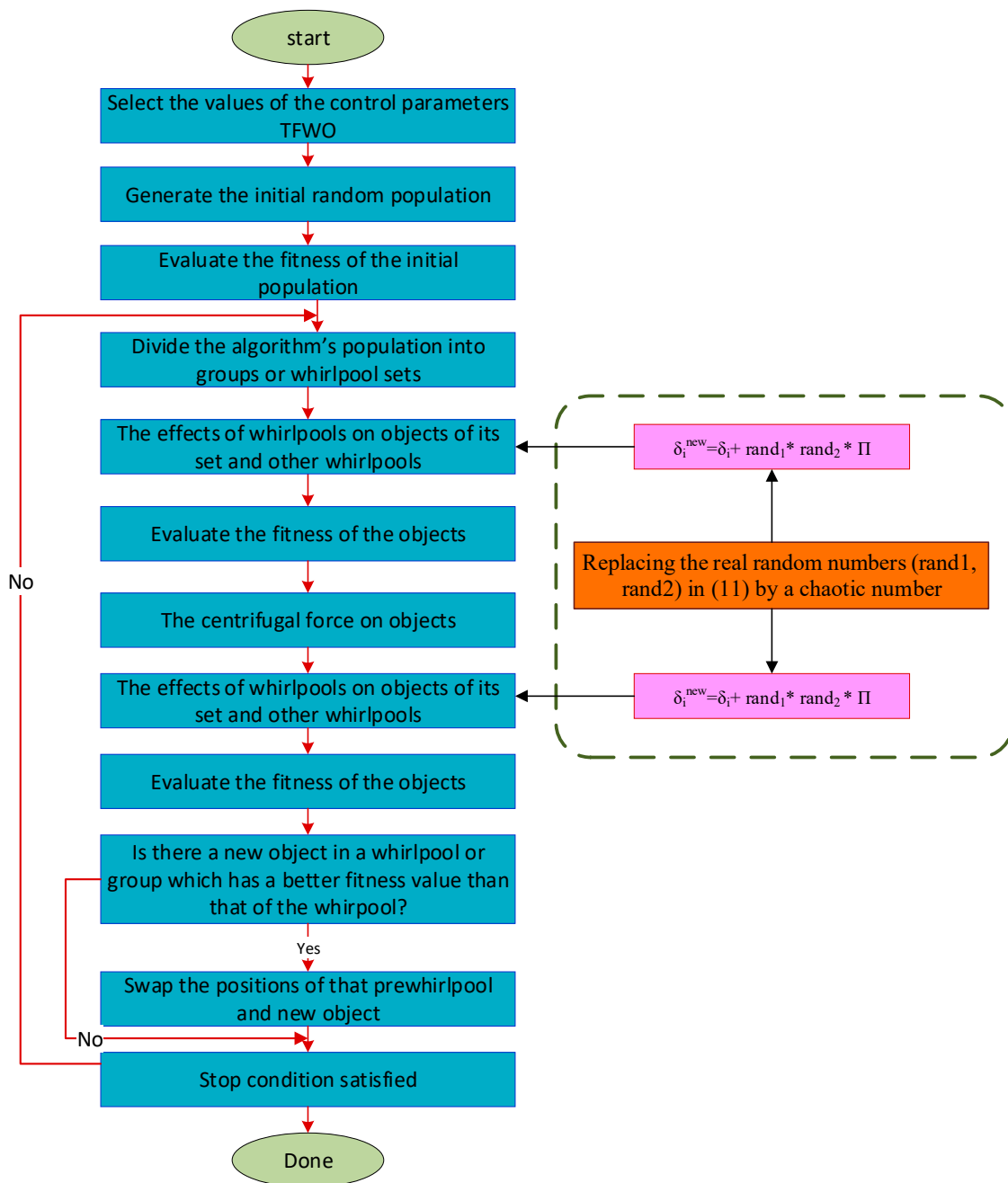


Figure 2. The proposed CTFWO algorithm flow chart.

4. Simulation Results and Discussion

The algorithms proposed in our study are applied to two different standard power systems (IEEE 30-bus and IEEE 57-bus test systems). Figure 3 displays the IEEE 30-bus system, while Table 1 presents the description of the two test power systems. The proposed technique uses MATLAB 2018a programming, and all sections of the simulations have been executed on a PC with a 2.40 GHZ frequency CPU, and the installed memory (RAM) is 4.0 GB.

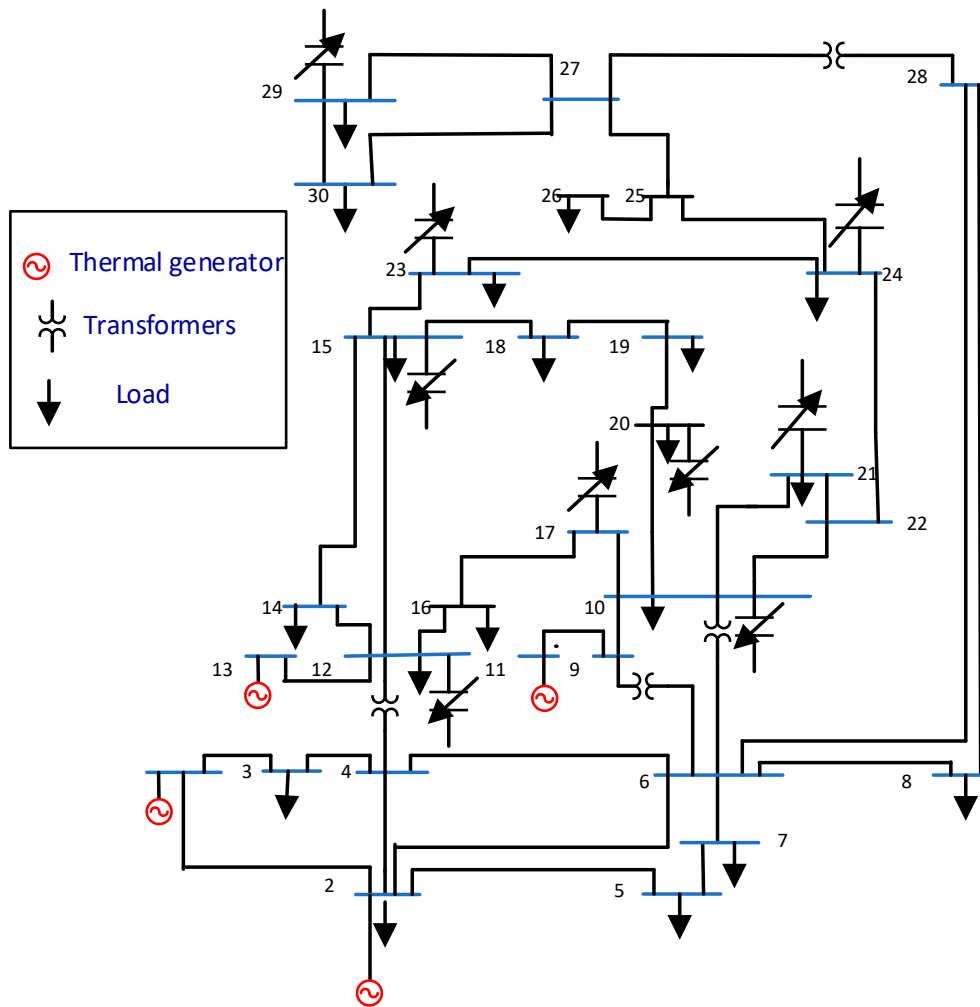


Figure 3. The IEEE 30-bus system.

Table 1. Description of test power systems.

Description	IEEE 30 Bus	IEEE 57 Bus
Buses, NB	30	57
Generators, NG	6	7
Transformers, NT	4	15
Shunts, NQ	9	3
Branches, NE	41	80
Equality constraints	60	114
Inequality constraints	125	245
Control variables	19	27
Discrete variables	6	20
Base case for P_{loss} , MW	5.660	27.8637
Base case for TVD, p.u.	0.58217	1.23358

The software used is MATLAB 2018, and our computer has a 2.67 GHz Intel Core i5 processor and 4 GB RAM. The results relating to the performance for all our algorithms are taken after many trials. In our study, we have taken the population size of 30, while the number of iterations is 500 in both tested systems. In Table 1, we show that the values produced by the CTFWO algorithm, in the case of power losses, are better and more optimal values compared with the other four algorithms for the IEEE 30-bus system. In Table 2, we show the generator voltage, transformer tap ratio, capacitor bank, and generator reactive power values for case one, which simulates power losses in the 30-bus system.

Table 2. Results of case 1 for the 30-bus system.

Parameters	Min	Max	Case 1 (Min Ploss)					
			AEO	EO	GBO	TFWO	CTFWO	
Generator voltage								
V1 (p.u.)	0.95	1.1	1.071383	1.071472	1.071032	1.071288	1.071342	
V2 (p.u.)	0.95	1.1	1.062422	1.062185	1.061796	1.062056	1.06216	
V5 (p.u.)	0.95	1.1	1.039959	1.039844	1.039846	1.039836	1.039794	
V8 (p.u.)	0.95	1.1	1.040165	1.039817	1.039876	1.039847	1.039981	
V11 (p.u.)	0.95	1.1	1.029138	1.036577	1.032475	1.040013	1.031899	
V13 (p.u.)	0.95	1.1	1.060438	1.06159	1.062488	1.061949	1.062353	
Transformer tap ratio								
T11 (p.u.)	0.9	1.1	1.0131	0.996542	1.01535	0.992784	1.013433	
T12 (p.u.)	0.9	1.1	0.908055	0.926149	0.900161	0.93027	0.900373	
T15 (p.u.)	0.9	1.1	0.981065	0.982578	0.984448	0.983187	0.983546	
T36 (p.u.)	0.9	1.1	0.986214	0.986534	0.986786	0.986749	0.987144	
Capacitor bank								
QC10 (MVar)	0	5	2.578379	0.8186	0.521123	0	0.005125	
QC12 (MVar)	0	5	0.109959	0	0.260124	0	0	
QC15 (MVar)	0	5	4.465515	4.99961	4.99989	1.870626	1.870944	
QC17 (MVar)	0	5	1.942079	0.000254	0.080239	0.582313	0.792172	
QC20 (MVar)	0	5	0.672555	0.327968	1.739245	1.047382	4.978545	
QC21 (MVar)	0	5	2.894689	4.687609	0.509966	4.261626	2.360041	
QC23 (MVar)	0	5	3.222698	2.5062	4.03902	0	0.002876	
QC24 (MVar)	0	5	1.608914	4.962173	1.747189	4.089292	3.716173	
QC29 (MVar)	0	5	1.663508	3.687004	4.823309	0.000215	0	
Objective function								
Ploss (MW)	NA	NA	4.9449	4.944875	4.945	4.9449	4.9448	
Generator reactive power								
QG1 (MVar)	−29.8	59.6	−3.37149	−2.7178	−3.06773	−2.92771	−2.98714	
QG2 (MVar)	−24	48	12.04035	11.25537	10.63886	11.10803	11.47796	
QG5 (MVar)	−30	60	1.583144	1.733564	1.953514	1.785632	1.750684	
QG8 (MVar)	−26.5	53	26.77981	26.53406	26.73682	26.56385	27.28592	
QG11 (MVar)	−7.5	15	−5.89765	−5.28439	−4.32984	−4.53925	−4.66229	
QG13 (MVar)	−7.8	15.5	8.15796	9.03965	9.728283	9.315351	9.62484	

The best values obtained are in bold.

In Table 3, we show that the values for the CTFWO algorithm are better and more optimal compared with the other algorithms in the case of power losses in the IEEE 30-bus system. In Figure 4, the CTFWO algorithm gives the minimal values in the case of power losses compared to the other algorithms.

Table 3. Results of the first objective function for the IEEE 30-bus system.

	AEO	EO	GBO	TFWO	CTFWO
Worst	4.9473	4.94658	4.9755	4.9459	4.9453
Best	4.9449	4.944875	4.945	4.9449	4.94480
Median	4.94555	4.9453745	4.94635	4.94515	4.9449
Mean	4.945715	4.9455445	4.949695	4.945205	4.944915
Std.					
Deviation	0.000640	0.00051849	0.00797776	0.00024381	0.00010399

The best values obtained are in bold.

The voltage profiles of all the algorithms for the 30 buses in this system are illustrated in Figure 5. The figure shows that the voltages magnitudes for all buses are within the specified limits. However, the voltage profile in the case of using the proposed CTFWO technique has the better profile for most buses in the system than the other algorithms. Figure 6 shows the reactive power values of the six generators for the 30-bus power system in case one, which simulates power losses, for all algorithms.

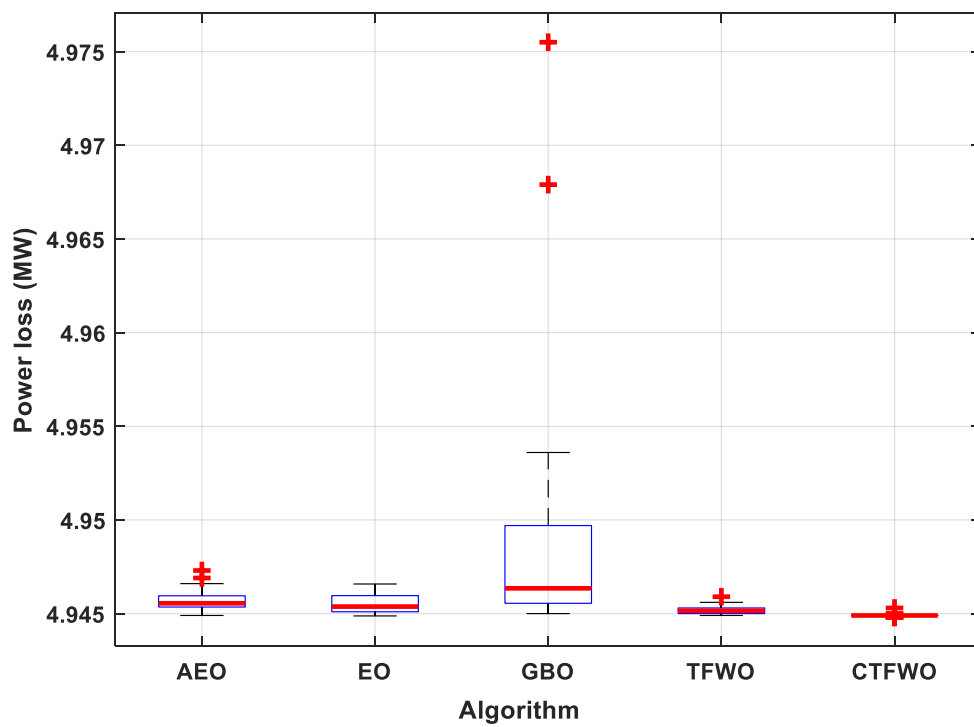


Figure 4. Boxplots for all algorithms for the 30-bus system in case 1.

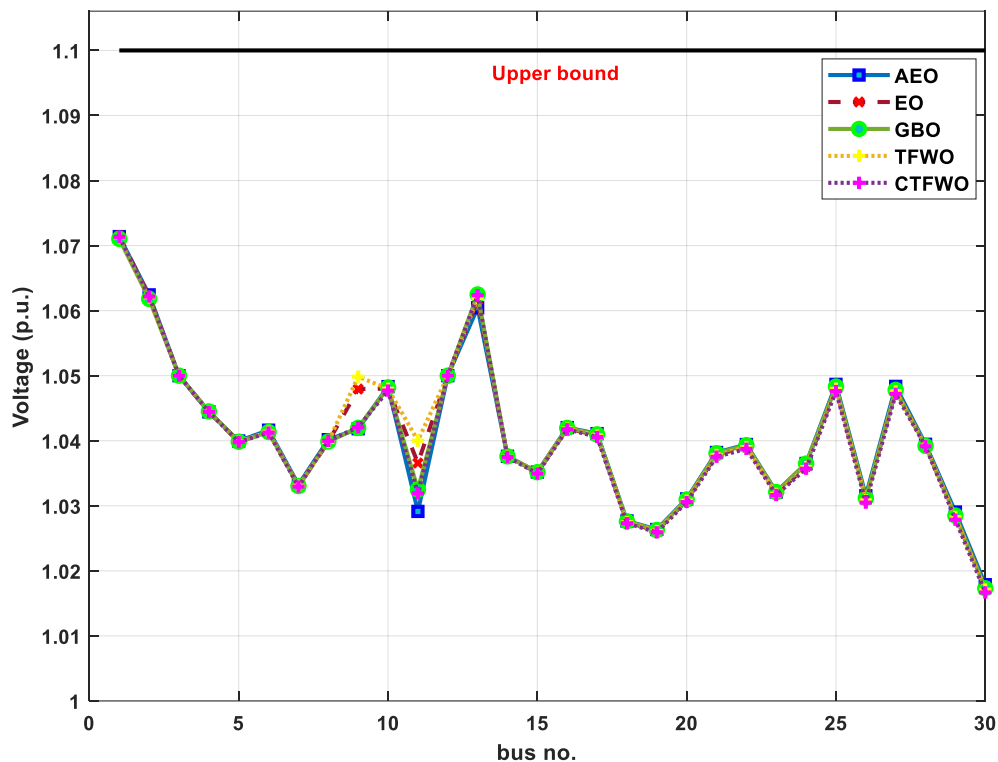


Figure 5. Voltage profiles of load bus for the 30-bus system in case 1.

In Table 4, the generator voltage, transformer tap ratio, capacitor bank, and generator reactive power values are shown for the voltage deviation simulation with the 30-bus system. Table 5 shows that the values obtained by the CTFWO algorithm are better and more optimal than those obtained by the others in the case of voltage deviation for the IEEE 30-bus system.

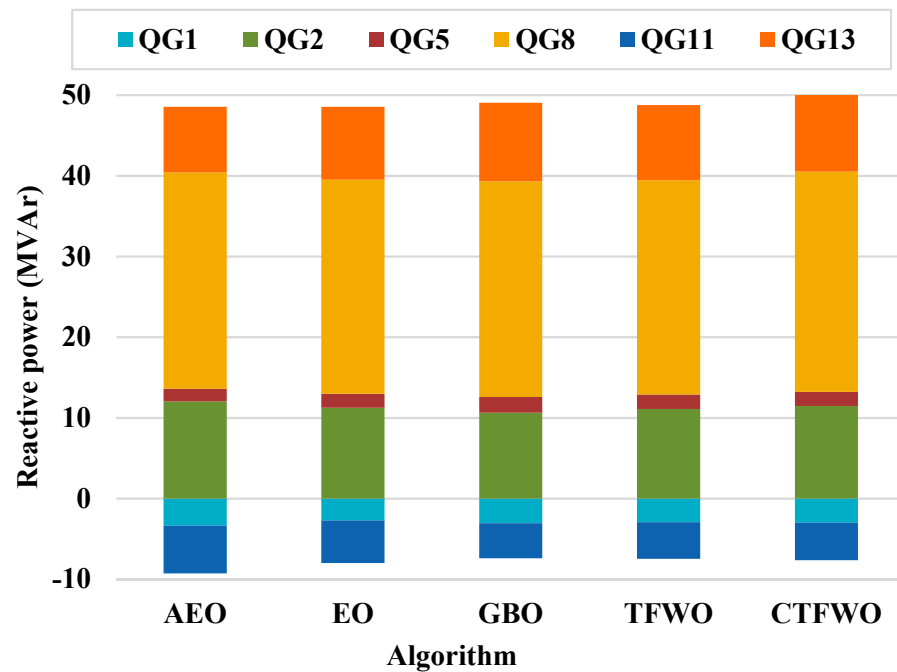


Figure 6. Representation of reactive power values of the generators for the 30-bus system in case 1.

Table 4. Results of case 2 for the 30-bus system.

Parameters	Min	Max	Case 2 (Min VD)				
			AEO	EO	GBO	TFWO	CTFWO
Generator voltage							
V1 (p.u.)	0.95	1.1	1.007321	1.004997	1.004141	1.006213	1.002472
V2 (p.u.)	0.95	1.1	1.008668	1.00445	1.004527	1.007222	1.002336
V5 (p.u.)	0.95	1.1	1.016353	1.017078	1.016646	1.017246	1.017129
V8 (p.u.)	0.95	1.1	1.004699	1.004935	1.005271	1.006619	1.006552
V11 (p.u.)	0.95	1.1	1.007415	1.003181	1.007753	0.986987	0.994936
V13 (p.u.)	0.95	1.1	1.018235	1.026852	1.027531	1.023421	1.033269
Transformer tap ratio							
T11 (p.u.)	0.9	1.1	1.041081	1.037017	1.039456	1.016957	1.025889
T12 (p.u.)	0.9	1.1	0.906165	0.900177	0.900001	0.907931	0.9
T15 (p.u.)	0.9	1.1	0.960256	0.975119	0.975975	0.968549	0.985956
T36 (p.u.)	0.9	1.1	0.969779	0.968731	0.970034	0.97011	0.969488
Capacitor bank							
QC10 (MVar)	0	5	4.081875	4.087516	1.027896	2.676166	1.742964
QC12 (MVar)	0	5	1.911945	0.964742	2.500364	2.653514	1.827241
QC15 (MVar)	0	5	2.438076	0.000256	0.000249	4.026815	0.007227
QC17 (MVar)	0	5	3.247676	4.911974	1.68685	2.796258	3.506281
QC20 (MVar)	0	5	3.134319	1.643454	1.376082	0	4.730291
QC21 (MVar)	0	5	4.002702	4.993874	4.776548	4.999999	2.19×10^{-6}
QC23 (MVar)	0	5	0.939362	0.04512	1.097063	0.803642	2.934356
QC24 (MVar)	0	5	3.314184	1.963021	4.074833	1.928107	0.020687
QC29 (MVar)	0	5	1.517154	1.885478	3.257629	0.001063	3.853446
Objective function							
VD (p.u.)	NA	NA	0.12308	0.122428	0.12202	0.12206	0.12127
Generator reactive power							
QG1 (MVar)	-29.8	59.6	-29.799	-27.7386	-29.8	-29.8	-29.7778
QG2 (MVar)	-24	48	4.050136	-6.40245	-4.69091	0.917091	-9.34062
QG5 (MVar)	-30	60	27.13882	30.35612	29.72286	29.12533	31.54037
QG8 (MVar)	-26.5	53	38.5871	40.69673	40.73791	45.66735	45.28808
QG11 (MVar)	-7.5	15	4.004549	1.949049	4.169385	-5.75336	-2.00473
QG13 (MVar)	-7.8	15.5	4.203959	10.50824	11.02679	7.990866	15.27388

The best values obtained are in bold.

Table 5. Results of the second objective function for the IEEE 30-bus system.

	AEO	EO	GBO	TFWO	CTFWO
Worst	0.12811	0.128889	0.12655	0.12498	0.12365
Best	0.12308	0.122428	0.12202	0.12206	0.12127
Median	0.1244	0.124771	0.12379	0.12367	0.122195
Mean	0.124646	0.12517885	0.1238055	0.123365	0.122363
Std.	0.001245	0.00159252	0.00104612	0.000920	0.000794686
Deviation	0.001245	0.00159252	0.00104612	0.000920	0.000794686

The best values obtained are in bold.

In Figure 7, the CTFWO algorithm gives the lowest values in the case of voltage deviation compared to the other algorithms in the 30-bus power system.

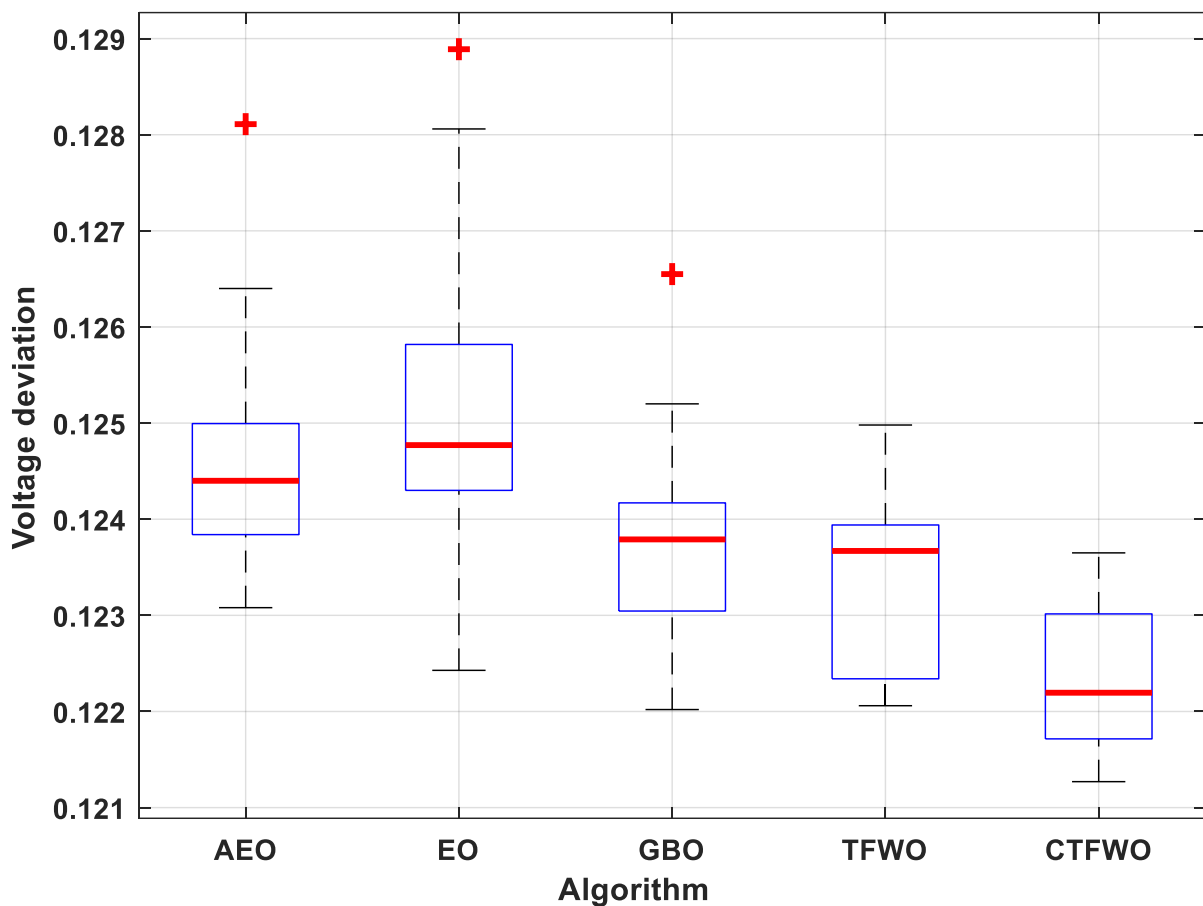


Figure 7. Boxplots for all algorithms for the 30-bus system in case 2.

The voltage profiles in p.u. for all algorithms with the 30 buses in this system are illustrated in Figure 8. The figure shows that the voltages magnitudes for all the buses are within the specified limits. However, the voltage profile in the case of using the proposed CTFWO technique has the better profile for most buses in the system than other algorithms. Figure 9 shows the reactive power values of the six generators for the 30-bus power system in case two, which simulates the voltage deviation, for all the algorithms.

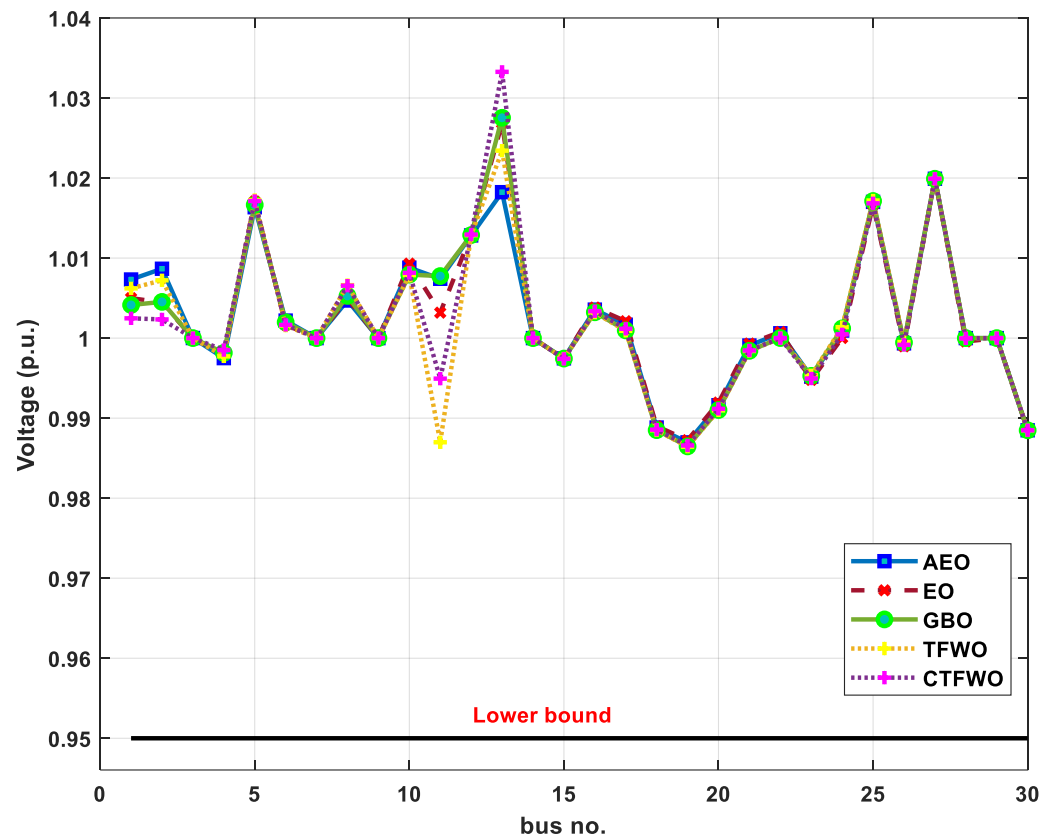


Figure 8. Voltage profiles of load bus for the 30-bus system in case 2.

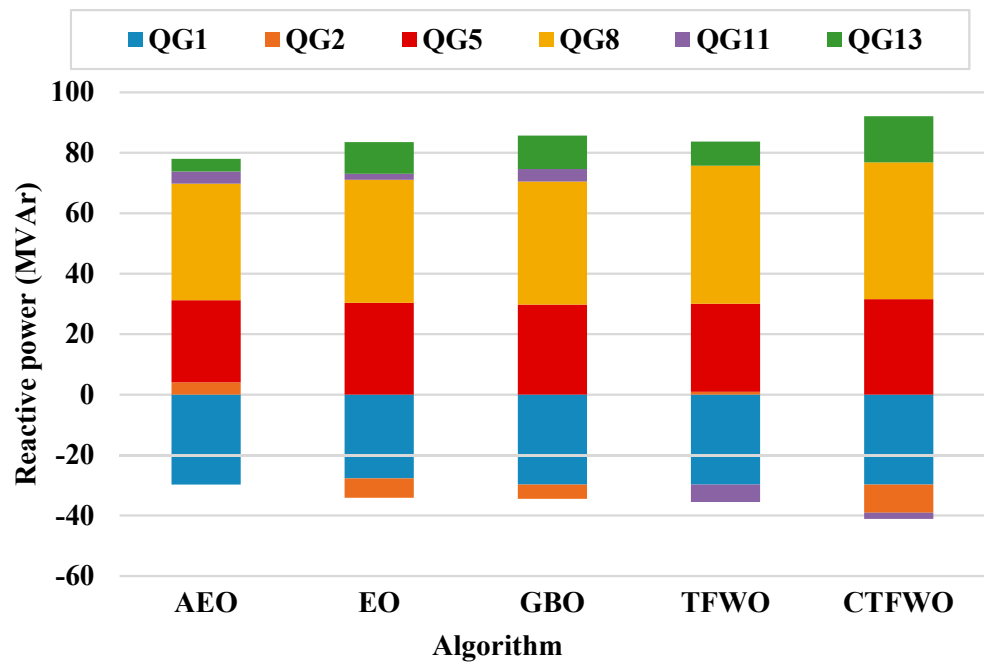


Figure 9. Representation of reactive power values of the generators for the 30-bus system in case 2.

Table 6 shows the generator voltage, transformer tap ratio, capacitor bank, and generator reactive power values for the power losses in the 57-bus power system.

Table 6. Results of case 3 for the IEEE 57-bus system.

Parameters	Min	Max	Case 3 (Min Ploss)				
			AEO	EO	GBO	TFWO	CTFWO
Generator voltage							
V1 (p.u.)	0.95	1.1	1.084262	1.088584	1.083097	1.088347	1.086947
V2 (p.u.)	0.95	1.1	1.073155	1.076589	1.072353	1.076389	1.076199
V3 (p.u.)	0.95	1.1	1.060508	1.061101	1.060881	1.060936	1.064546
V6 (p.u.)	0.95	1.1	1.054363	1.05593	1.054203	1.052998	1.055437
V8 (p.u.)	0.95	1.1	1.072266	1.074526	1.07583	1.069332	1.075181
V9 (p.u.)	0.95	1.1	1.043366	1.040742	1.046384	1.03933	1.043497
V12 (p.u.)	0.95	1.1	1.051094	1.043244	1.053073	1.044047	1.046439
Transformer tap ratio							
T19 (p.u.)	0.9	1.1	19.89077	13.69412	7.408436	9.135741	8.562415
T20 (p.u.)	0.9	1.1	10.16505	15.49922	10.68707	8.746681	15.89978
T31 (p.u.)	0.9	1.1	11.50229	13.62317	10.5197	10.15296	13.51124
T35 (p.u.)	0.9	1.1	19.99983	4.99742	8.079208	8.39333	9.863767
T36 (p.u.)	0.9	1.1	3.869202	15.18321	12.87629	18.10179	8.393917
T37 (p.u.)	0.9	1.1	16.57872	10.01611	9.812319	10.48957	10.46434
T41 (p.u.)	0.9	1.1	15.42004	9.173277	9.720015	9.478536	9.601751
T46 (p.u.)	0.9	1.1	5.798275	3.498912	4.356667	5.942918	4.812247
T54 (p.u.)	0.9	1.1	14.06045	0.000382	8.26881	5.02964	6.24×10^{-1}
T58 (p.u.)	0.9	1.1	8.591331	8.13231	8.255977	8.793688	8.864324
T59 (p.u.)	0.9	1.1	7.440277	8.03943	9.558948	6.840257	7.132084
T65 (p.u.)	0.9	1.1	9.010086	8.982809	10.26309	7.232212	7.519419
T66 (p.u.)	0.9	1.1	4.49412	4.778383	5.390395	3.8371	4.15625
T71 (p.u.)	0.9	1.1	7.729125	9.197826	6.989455	6.203619	7.338977
T73 (p.u.)	0.9	1.1	14.15773	1.179605	10.40507	10.28327	8.63043
T76 (p.u.)	0.9	1.1	10.54353	5.89709	6.67063	7.707681	5.909717
T80 (p.u.)	0.9	1.1	14.3393	7.510371	9.155039	8.080104	8.890491
Capacitor bank							
QC18 (MVar)	0	20	24.44492	12.17391	8.353978	7.752999	12.36848
QC25 (MVar)	0	20	16.00438	14.4781	14.66842	16.74156	11.78276
QC53 (MVar)	0	20	16.51053	1.745298	15.49276	15.08808	14.34732
Objective function							
Ploss (MW)	NA	NA	23.4554	23.68991	23.4998	23.3654	23.3235
Generator reactive power							
QG1 (MVar)	−140	200	46.0987	64.86378	40.53132	62.32991	51.02177
QG2 (MVar)	−17	50	49.99321	49.89506	49.99514	50	49.99121
QG3 (MVar)	−10	60	28.60956	35.96237	42.07875	38.02165	45.49167
QG6 (MVar)	−8	25	−3.05249	4.164812	−2.94065	1.498968	−3.36924
QG8 (MVar)	−140	200	60.07686	76.3103	66.07949	59.34457	69.22393
QG9 (MVar)	−3	9	8.999705	8.943546	8.999614	8.999999	8.999902
QG12 (MVar)	−150	155	64.08973	43.69682	65.40404	47.77938	49.32905

The best values obtained are in bold.

In Table 7, we observe that the CTFWO algorithm gives better, more optimal values in the case of power losses for the 57-bus system than those obtained from the other algorithms.

Table 7. Results of the first objective function for the IEEE 57-bus system.

	AEO	EO	GBO	TFWO	CTFWO
Worst	24.1993	27.12346	23.8371	25.201	24.9111
Best	23.4554	23.68991	23.4998	23.3654	23.3235
Median	23.5902	25.03884	23.61985	23.7303	23.4988
Mean	23.683825	25.368013	23.63577	23.833395	23.639485
Std. Deviation	0.24361589	1.055693	0.10222382	0.4940579	0.38384166

The best values obtained are in bold.

In Figure 10, we see that the CTFWO algorithm gives the best values at all individual runs in the case of power losses compared to the other algorithms for the 57-bus power system.

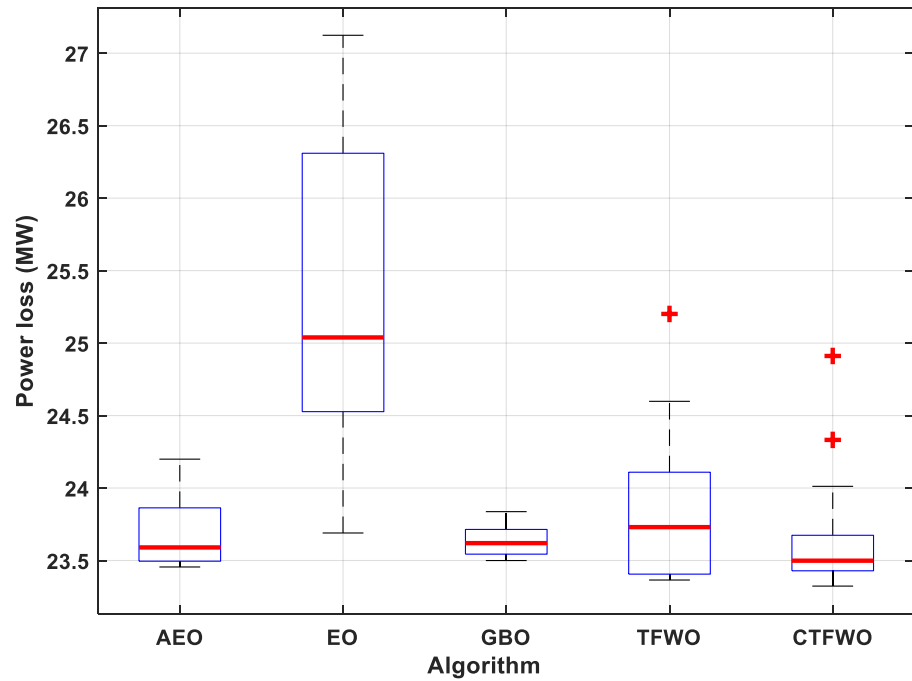


Figure 10. Boxplots for all algorithms for the 57-bus system in case 3.

The voltage profiles in p.u. for all the algorithms for the 57 buses in this system are illustrated in Figure 11. The figure shows that the voltages magnitudes for all the buses are within the specified limits. However, the voltage profile in the case of using the proposed CTFWO technique has the better profile for most buses in the system than the other algorithms. Figure 12 shows the reactive power values in the 57-bus power system in case three, which simulates voltage deviation, for all the algorithms.

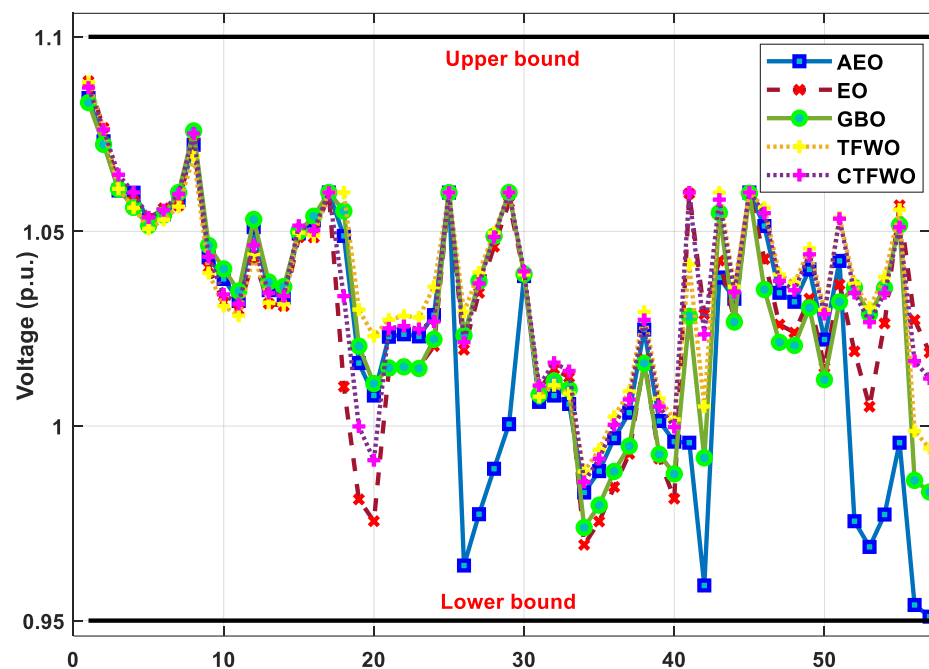


Figure 11. Voltage profiles of load bus for the 57-bus system in case 3.

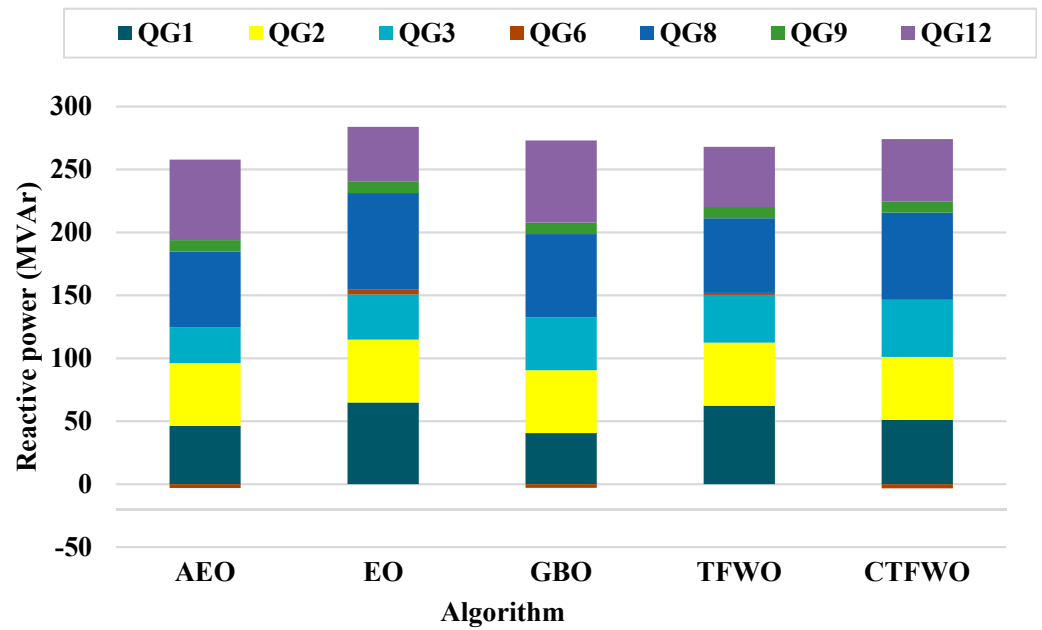


Figure 12. Representation of reactive power values of the generators for the 57-bus system in case 3.

Table 8 illustrates the generator voltage, transformer tap ratio, capacitor bank and generator reactive power values for the case of voltage deviation in the 57-bus system.

Table 8. Results of case 4 for the IEEE 57-bus system.

Parameters	Min	Max	Case 4 (Min VD)				
			AEO	EO	GBO	TFWO	CTFWO
Generator voltage							
V1 (p.u.)	0.95	1.1	1.021242	1.013827	1.027151	1.031907	1.014437
V2 (p.u.)	0.95	1.1	1.009187	1.006551	1.016181	1.021767	1.006477
V3 (p.u.)	0.95	1.1	1.012401	1.009924	1.008498	1.014731	1.012832
V6 (p.u.)	0.95	1.1	1.001737	1.003425	1.003667	1.001059	1.008131
V8 (p.u.)	0.95	1.1	1.01807	1.023622	1.017704	1.003394	1.030427
V9 (p.u.)	0.95	1.1	0.998958	0.99855	0.998712	0.989075	1.008076
V12 (p.u.)	0.95	1.1	1.032864	1.018975	1.029294	1.021346	1.034201
Transformer tap ratio							
T19 (p.u.)	0.9	1.1	15.41972	19.80841	4.345691	15.27412	10.61522
T20 (p.u.)	0.9	1.1	11.05992	8.455433	13.30462	7.826019	15.278
T31 (p.u.)	0.9	1.1	7.143219	7.227283	7.110257	7.249017	7.372825
T35 (p.u.)	0.9	1.1	19.65228	17.31383	12.17408	10.53058	17.76376
T36 (p.u.)	0.9	1.1	13.44046	19.99667	17.53505	19.99013	20
T37 (p.u.)	0.9	1.1	10.13173	11.21114	10.83356	9.719896	10.79664
T41 (p.u.)	0.9	1.1	10.82383	11.1787	9.627105	9.317074	10.74971
T46 (p.u.)	0.9	1.1	2.413594	3.985416	4.097224	1.68163	1.734963
T54 (p.u.)	0.9	1.1	0.032358	0.00	0.000183	2.26×10^{-6}	0.00
T58 (p.u.)	0.9	1.1	3.247924	4.735199	2.983137	2.993189	2.95414
T59 (p.u.)	0.9	1.1	5.955591	6.472745	8.943067	5.794069	8.938434
T65 (p.u.)	0.9	1.1	9.137057	8.268309	10.09535	9.793917	11.07804
T66 (p.u.)	0.9	1.1	2.069724	0.419808	2.11×10^{-6}	0.00	0.00
T71 (p.u.)	0.9	1.1	7.471875	5.29712	6.490749	4.988462	6.106468
T73 (p.u.)	0.9	1.1	5.314451	10.0823	9.159237	9.145331	10.33043
T76 (p.u.)	0.9	1.1	1.800253	0.00	4.71×10^{-5}	0.00	0.00
T80 (p.u.)	0.9	1.1	9.097109	9.074298	8.345625	9.10713	10.86881

Table 8. Cont.

Parameters	Min	Max	Case 4 (Min VD)					
			AEO	EO	GBO	TFWO	CTFWO	
Capacitor bank								
QC18 (MVar)	0	20	18.26974	19.07913	4.726816	9.512274	19.13888	
QC25 (MVar)	0	20	22.14967	26.64133	23.11284	17.50151	21.75597	
QC53 (MVar)	0	20	27.88595	27.89456	22.68993	28.56028	27.37095	
			Objective function					
VD (p.u.)	NA	NA	0.60495	0.596804	0.60383	0.58588	0.58553	
Generator reactive power								
QG1 (MVar)	−140	200	3.364011	−13.2065	12.58937	23.46288	−24.2855	
QG2 (MVar)	−17	50	31.87596	49.2699	47.99061	49.97456	43.33627	
QG3 (MVar)	−10	60	59.6576	58.89933	43.98599	59.99735	58.95072	
QG6 (MVar)	−8	25	−6.96418	−7.98727	6.681949	10.26215	−7.99952	
QG8 (MVar)	−140	200	28.2041	44.74489	28.10331	3.612073	44.07484	
QG9 (MVar)	−3	9	2.601341	8.979909	8.692275	8.999975	8.999156	
QG12 (MVar)	−150	155	153.8968	127.2061	140.3891	126.7261	152.9637	

The best values obtained are in bold.

Table 9 shows that the CTFWO algorithm gives better and more optimal values for the 57-bus system in the case of voltage deviation compared with the other algorithms.

Table 9. Results of the second objective function for the IEEE 57-bus system.

	AEO	EO	GBO	TFWO	CTFWO
Worst	0.68792	1.067937	0.72276	0.69456	0.61783
Best	0.60495	0.596804	0.60383	0.58588	0.58553
Median	0.64876	0.718362	0.63507	0.614465	0.593385
Mean	0.6489715	0.7751617	0.639779	0.622149	0.596695
Std. Deviation	0.02736555	0.14116848	0.02654973	0.02774483	0.011368281

The best values obtained are in bold.

In Figure 13, the CTFWO algorithm gives the best values at 30 individual runs in the case of voltage deviation compared to the other algorithms in the 57-bus power system.

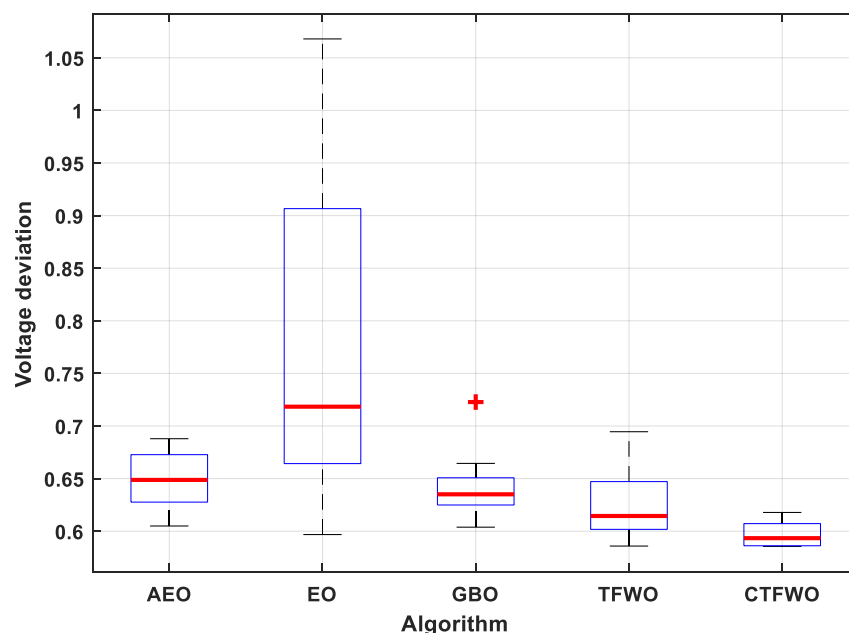


Figure 13. Boxplots for all algorithms for the 57-bus system in case 4.

The voltage profiles in p.u. for all the algorithms for the 57 buses in this system are illustrated in Figure 14. The figure shows that the voltages magnitudes for all the buses are within the specified limits. However, the voltage profile in the case of using the proposed CTFWO technique has the better profile for most buses in the system than the other algorithms. Figure 15 shows the reactive power values in the 57-bus power system in case four, which simulates voltage deviation, for all the algorithms.

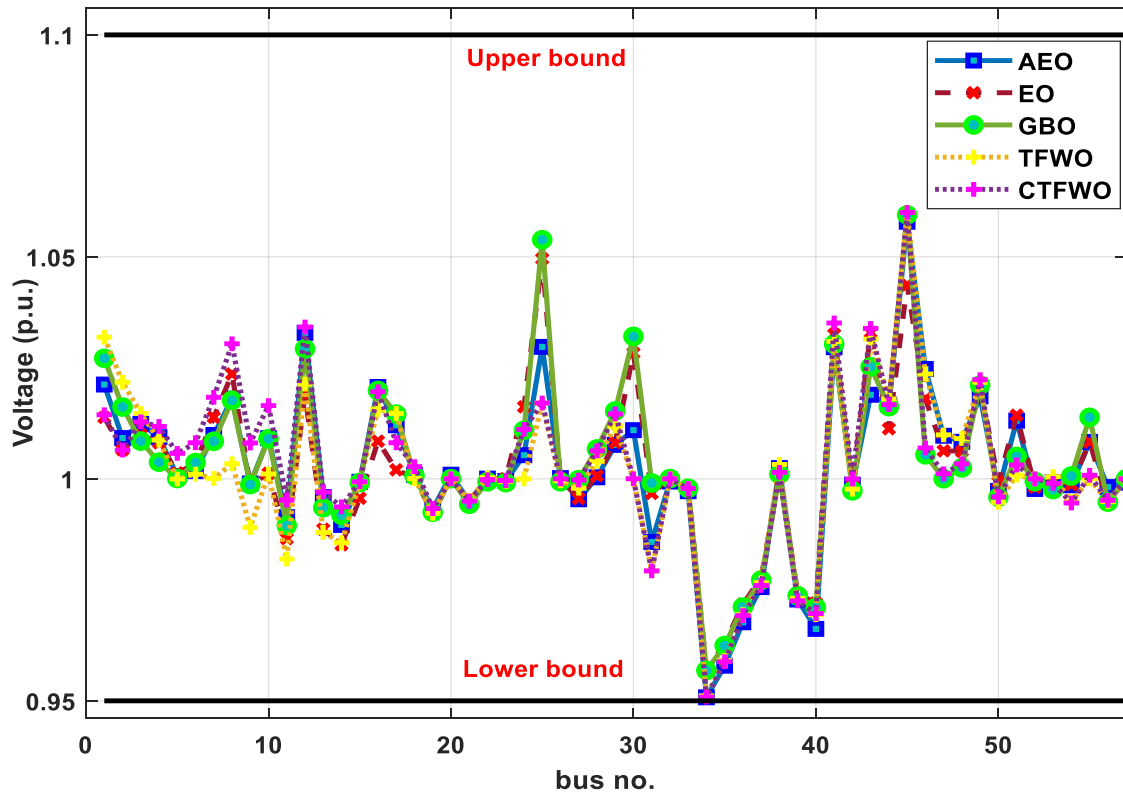


Figure 14. Voltage profiles of load bus for the 57-bus system in case 4.

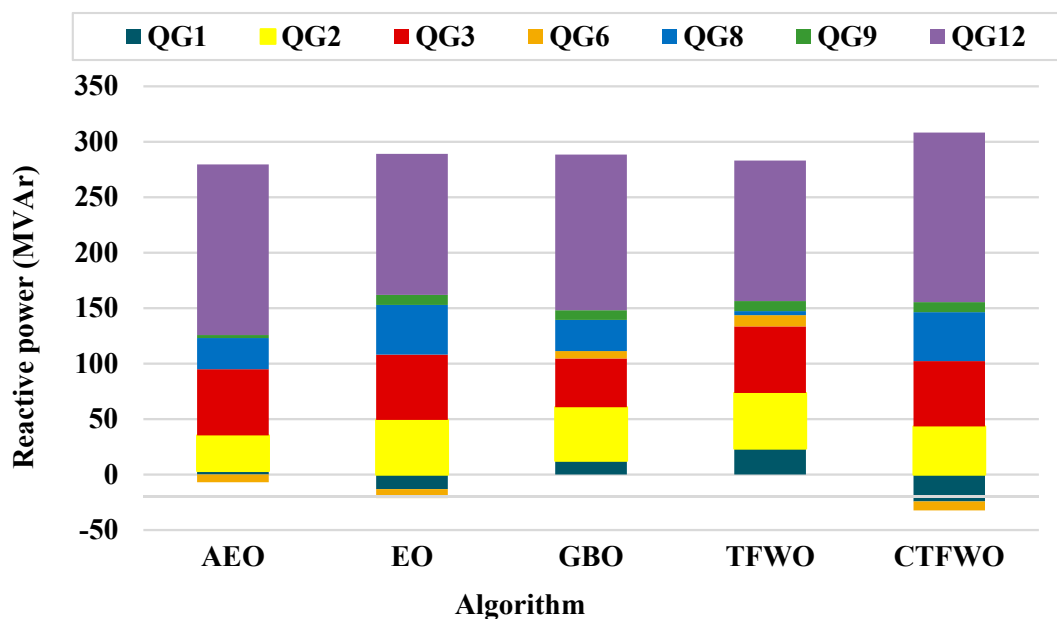


Figure 15. Representation of reactive power values of the generators for the 57-bus system in case 4.

In the case of the 30-bus power system and the 57-bus power system, we performed 30 different trials for each algorithm under study and recorded the best trial for each one and plotted them as shown in Figures 16–19.

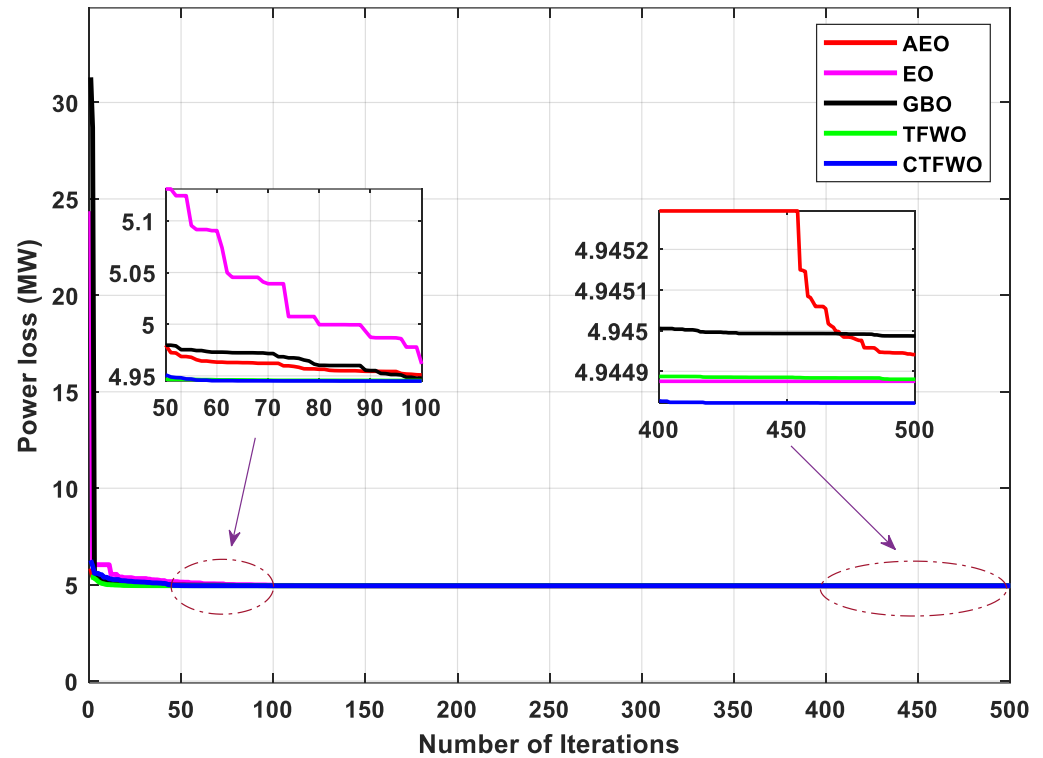


Figure 16. Power loss (P_{loss}) with number of iterations for the 30-bus power system.

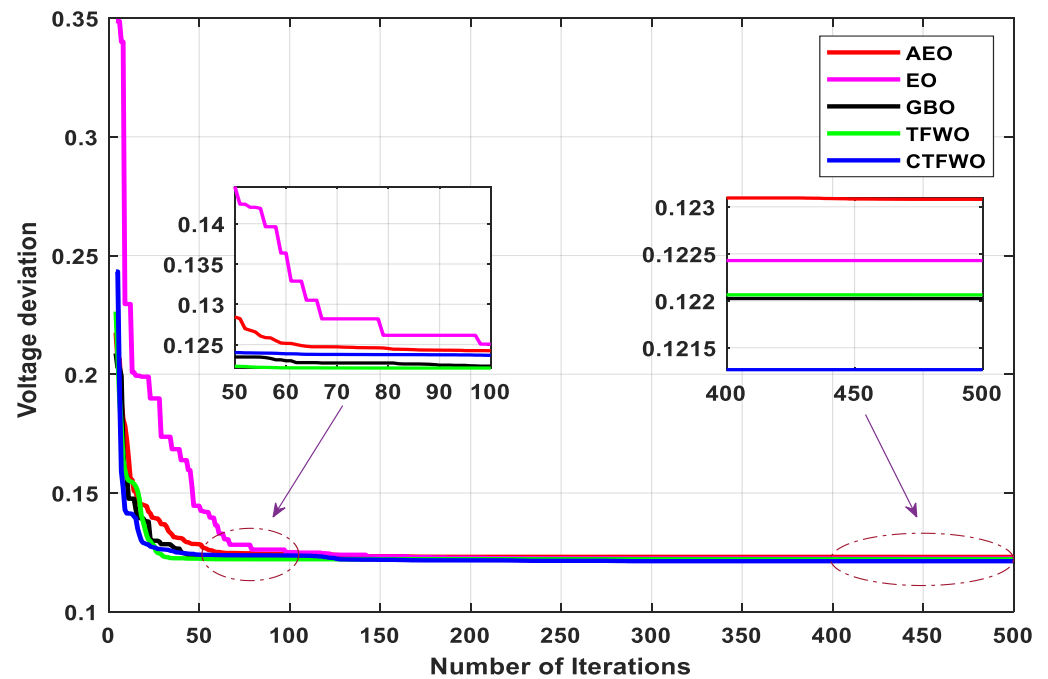


Figure 17. Voltage deviation (VD) with number of iterations for the 30-bus power system.

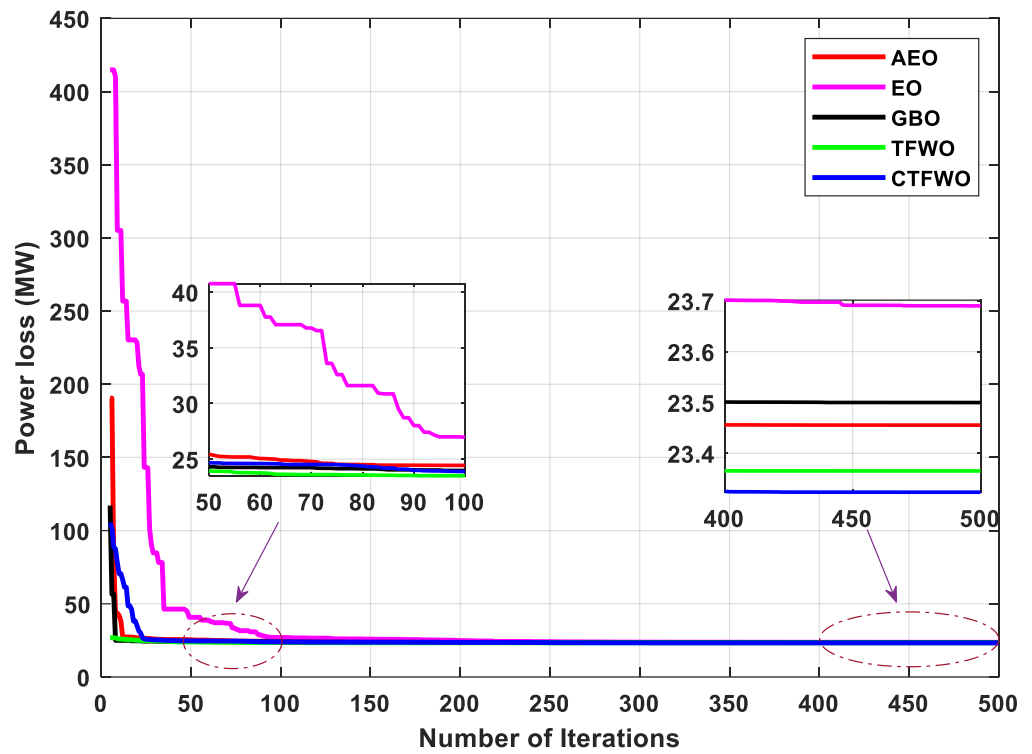


Figure 18. Power loss (P_{loss}) with number of iterations for the 57-bus power system.

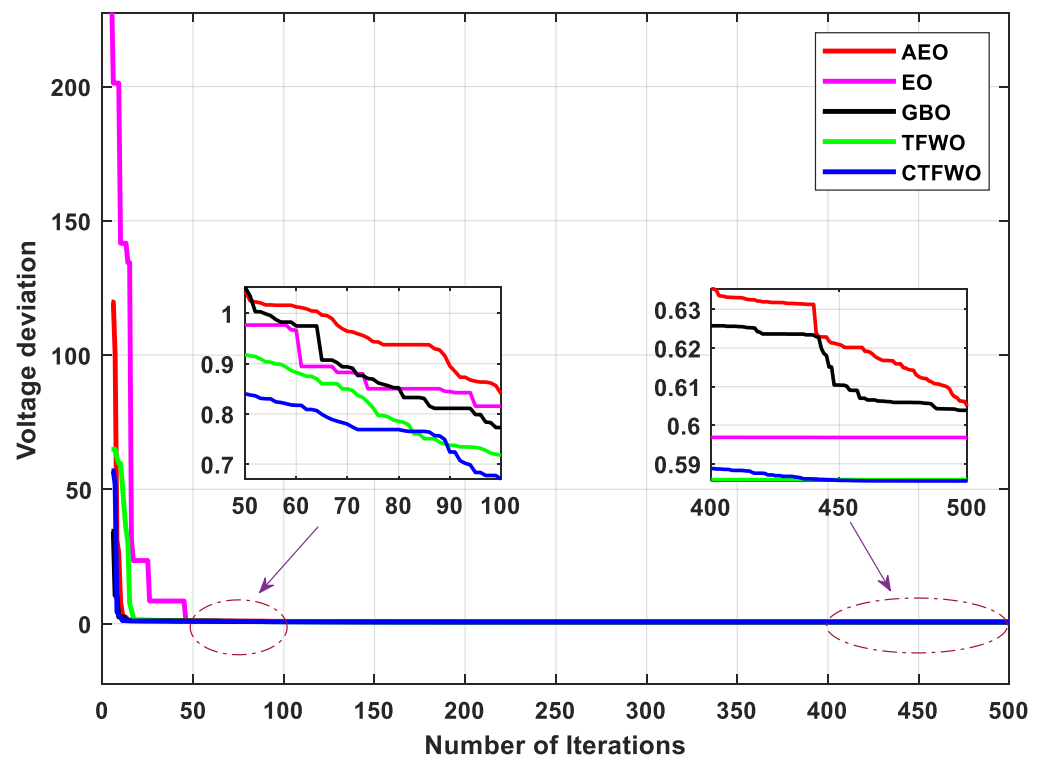


Figure 19. Voltage deviation (VD) with number of iterations for the 57-bus power system.

Figures 16 and 17 illustrate the curves in the case of power loss and voltage deviation for the 30-bus power system, and from these we can see that the CTFWO algorithm achieves the best, most minimal, smoothest, lowest curve compared with the other algorithms.

Figures 18 and 19 illustrate the curves in the case of power loss and voltage deviation for the 57-bus power system and from these we can see that the CTFWO algorithm achieves the best, most minimal, smoothest, lowest curve compared with the other algorithms.

The values for power loss for the 30-bus system vary from 4.945 (in GBO) to 4.9449 (in TFWO); however, after using our algorithm (CTFWO), it becomes 4.94480. In addition, for the 57-bus system variation, it ranges from 23.68991 (in EO) to 23.3654 (in TFWO); however, after using our algorithm (CTFWO), it becomes 23.3235. Moreover, the values for voltage deviation for the 30-bus system is vary from 0.12308 (in AEO) to 0.12206 (in TFWO); by using our algorithm (CTFWO), it becomes 0.12127. Finally, for the 57-bus system variation, the values range from 0.60495 (in AEO) to 0.58588 (in TFWO); however, after using our algorithm (CTFWO), it becomes 0.58553.

Table 10 illustrates that the best result for power loss for the 30-bus system is produced by the CTFWO algorithm when compared with the other algorithms, as shown in the table.

Table 10. Comparison of results for power loss in the 30-bus system.

Test System	Min	Mean
SF-DE [65]	4.946	4.947
SP-DE [65]	4.947	4.9667
EC-DE [65]	4.946	4.9467
SR-DE [65]	4.946	4.9481
ECHT-DE [65]	4.947	4.9499
ALC-PSO [20]	5.1861	-
EB [40]	4.963	-
QODE [33]	5.2953	-
PSOGWO [68]	5.09037	-
CKHA [54]	5.1163	-
GA [68]	5.0977	-
OGSA [20]	5.1676	-
PSO [68]	5.1041	-
AEO	4.9449	4.945715
EO	4.944875	4.945545
GBO	4.945	4.949695
TFWO	4.9449	4.945205
CTFWO	4.9448	4.944915

In Table 11, we can observe that the best result for voltage deviation for the 30-bus system is produced by the CTFWO algorithm when compared with the other algorithms, as shown in the table.

Table 11. Comparison of results for voltage deviation in the 30-bus system.

Test System	Min	Mean
SF-DE [65]	0.1231	0.1243
SP-DE [65]	0.1224	0.1238
EC-DE [65]	0.1217	0.1235
SR-DE [65]	0.123	0.1241
ECHT-DE [65]	0.1229	0.1239
PGSWT-PSO [26]	0.1539	0.2189
PSO-TVAC [26]	0.2064	0.2376
GA [68]	0.3732	-
SPSO-TVAC [26]	0.1354	0.1558
PSO [68]	0.2816	-
SWT-PSO [26]	0.1614	0.1814
PSOGWO [68]	0.278	-
PSO-CF [26]	0.1287	0.1557
AEO	0.12308	0.124646
EO	0.122428	0.125179
GBO	0.12202	0.123806
TFWO	0.12206	0.123365
CTFWO	0.12127	0.122363

Table 12 shows that the best result for power loss is produced by the CTFWO algorithm when compared with the other algorithms for the 57-bus system.

Table 12. Comparison of results for power loss in the 57-bus system.

Test System	Min	Mean
SF-DE [65]	23.363	23.7164
SP-DE [65]	23.35	23.6956
EC-DE [65]	23.34	23.792
SR-DE [65]	23.355	23.4392
ECHT-DE [65]	23.396	23.4963
PSO [44]	24.3826	-
PGA [16]	23.836	24.5448
MCBOA [44]	23.6943	-
PSO-ICA [21]	24.1386	-
BA [40]	24.9254	-
BSO [69]	24.3744	-
MOGWA [43]	23.71544	-
ALC-PSO [20]	23.39	23.41
GSA [44]	24.4922	-
ICA [21]	24.1607	-
CSA [44]	24.2619	-
MOALO [70]	26.593	-
MFOM [40]	24.25293	-
WCA [51]	24.82	-
FPA [40]	24.8419	-
AEO	23.4554	23.68383
EO	23.68991	25.36801
GBO	23.4998	23.63577
TFWO	23.3654	23.8334
CTFWO	23.3235	23.63949

Table 13 shows that the results of the CTFWO algorithm for voltage deviations in the 57-bus system are the best compared with the other techniques.

Table 13. Comparison of results for voltage deviation in the 57-bus system.

Test System	Min	Mean
SF-DE [65]	0.586	0.6077
SP-DE [65]	0.589	0.6085
EC-DE [65]	0.59	0.6173
SR-DE [65]	0.59	0.6069
ECHT-DE [65]	0.588	0.6073
ALC-PSO [20]	0.6634	0.6689
NGWCA [51]	0.6501	-
BA [71]	0.6434	0.6499
OGSA [72]	0.6982	-
CBA-III [71]	0.6413	0.644
WCA [51]	0.6631	-
ALO [73]	0.6666	0.7534
CBA-IV [71]	0.6399	0.6424
GBWCA [51]	0.6501	-
AEO	0.60495	0.648972
EO	0.596804	0.775162
GBO	0.60383	0.639779
TFWO	0.58588	0.622149
CTFWO	0.58553	0.596695

The comparative Tables 10–13 show that from among the different optimized algorithms, the proposed algorithm (CTFWO) has clear advantages over the others, because it

achieves the best, most minimal values for power losses and voltage deviations, while also achieving the smoothest and lowest curves.

5. Conclusions

In this paper, several optimization algorithms; artificial ecosystem-based optimization, the equilibrium optimizer, the gradient-based optimizer, turbulent flow of water-based optimization, and proposed CTFWO are applied as tools to solve the ORPD problem by minimizing the voltage deviation (VD) and total transmission power loss (p_{loss}) in two standard power systems, a 30-bus system and a 57-bus system. For example, the values of power loss for the 30-bus system varied from 4.945 (in GBO) to 4.9449 (in TFWO), but after using our algorithm (CTFWO), it became 4.94480. Additionally, for the 57-bus system, there was variation from 23.68991 (in EO) to 23.3654 (in TFWO), but after using the proposed algorithm (CTFWO), it became 23.3235. Moreover, the values for voltage deviation in the 30-bus system varied from 0.12308 (in AEO) to 0.12206 (in TFWO); by using the proposed algorithm (CTFWO), it became 0.12127. For the 57-bus system variation, these values ranged from 0.60495 (in AEO) to 0.58588 (in TFWO); after using the proposed algorithm (CTFWO), it became 0.58553. From the all above results and discussions, we find that the CTFWO algorithm gives better voltage deviation and transmission power loss values than other algorithms, and that these results are also better than the results of other recently developed algorithms, such as the many modifications of the DE algorithm, PGSWT-PSO, OGSA, WCA, and GBWCA. The results that we obtained by using the proposed CTFWO algorithm are encouraging for future research. In the future, the proposed CTFWO can be used to solve ORPD problems for systems with a large number of buses, and also to study multi-objective ORPD problems.

Author Contributions: Conceptualization, S.K. and M.H.H.; Data curation, S.K. and M.H.H.; Formal analysis, S.K. and M.H.H.; Investigation, A.M.A.-E.W., S.K. and M.H.H.; Methodology, A.M.A.-E.W., S.K. and M.H.H.; Project administration, T.A.A. and M.I.M.; Resources, T.A.A. and M.I.M.; Software, S.K., M.H.H., T.A.A. and M.I.M.; Supervision, S.K., T.A.A. and M.I.M.; Validation, S.K. and M.H.H.; Visualization, T.A.A. and M.I.M.; Writing—original draft, A.M.A.-E.W., S.K. and M.H.H.; Writing—review & editing, T.A.A. and M.I.M. All authors have read and agreed to the published version of the manuscript.

Funding: This research received no external funding.

Institutional Review Board Statement: Not applicable.

Informed Consent Statement: Not applicable.

Data Availability Statement: Not applicable.

Conflicts of Interest: The authors declare no conflict of interest.

Abbreviations

ABC	Artificial bee colony algorithm	ACO	Ant colony optimization
AEO	Artificial ecosystem-based optimization	ALC-PSO	PSO with an aging leader and challengers
ABC-FF	ABC with firefly algorithm	ALO	Ant lion optimizer
AGA	Adaptive genetic algorithm	CKHA	Chaotic krill herd algorithm
CSA	Cuckoo search algorithm	CLPSO	PSO with comprehensive learning
CSOA	Crow search optimization algorithm	DE	Differential evolution
DSA	Differential search algorithm	DE-AS	Combination of DE and ant system method
EC	E-constraint	EO	Equilibrium optimizer algorithm
ECHT	Ensemble of constraint handling techniques	EMOA	Exchange market optimization algorithm
GA	Genetic algorithm	GBBWCA	Gaussian bare-bones water cycle algorithm

GBTLBO	Gaussian bare-bones-based TLBO algorithm	GBO	Gradient-based optimizer
GSA	Gravitational search algorithm	GWO	Gray wolf optimizer
HFA-NMS	Hybrid firefly algorithm-based Nelder–Mead simplex	HPSO	Hybrid PSO
HPSO-ICA	PSO hybrid and imperialist competitive algorithms	HPSO-TS	Hybrid PSO and tabu search method
HAS	Harmony search algorithm	ICA	Imperialist competitive algorithms
ICBO	Improved colliding bodies optimization	ICOA	Improved coyote optimization algorithm
ICSA	Improved CSA	JA	Jaya algorithm
MFO	Moth–flame optimization technique	MGBTLBO	Modified GBTLBO
MOGWA	Multi-objective grey wolf algorithm	MTLA-DDE	Hybrid modified teaching–learning technique and double differential evolution algorithm
ORPD	Optimal reactive power dispatch	OPF	Optimal power flow
PSO	Particle swarm optimization	PSO-GT	Combination of PSO and graph theory
PSO-IPG	PSO with pseudo-gradient theory and constriction factor	QODE	Quasi-oppositional differential evolution
QOTLBO	Quasi-oppositional teaching–learning based optimization	RCGA	Real coded genetic algorithm
SARCGA	Self-adaptive real coded genetic algorithm	SGA	Specialized genetic algorithm
Std. dev.	Standard deviation	SF	Superiority of feasible solutions
SP	Self-adaptive penalty	SR	Stochastic ranking
TFWO	Turbulent flow of water-based optimization	TLBO	Teaching–learning-based optimization
P_{loss}	Active power losses	VD	Voltage deviation
WOA	Whale optimization algorithm		

References

- Nakawiro, W.; Erlich, I.; Rueda, J.L. A novel optimization algorithm for optimal reactive power dispatch: A comparative study. In Proceedings of the 2011 4th International Conference on Electric Utility Deregulation and Restructuring and Power Technologies (DRPT), Weihai, China, 6–9 July 2011. [\[CrossRef\]](#)
- Mandal, B.; Roy, P.K. Optimal reactive power dispatch using quasi-oppositional teaching learning based optimization. *Electr. Power Energy Syst.* **2013**, *53*, 123–134. [\[CrossRef\]](#)
- Zhukov, A.; Tomin, N.; Sidorov, D.; Kurbatsky, V.; Panasetsky, D. On-line power systems security assessment using data stream random forest algorithm modification. In *Innovative Computing, Optimization and Its Applications*; Springer: Cham, Switzerland, 2018; pp. 183–200.
- Zhang, Y.; Song, X.; Li, Y.; Zeng, Z.; Yong, C.; Sidorov, D.; Lv, X. Two-Stage Active and Reactive Power Coordinated Optimal Dispatch for Active Distribution Network Considering Load Flexibility. *Energies* **2020**, *13*, 5922. [\[CrossRef\]](#)
- Voropai, N.I.; Tomin, N.V.; Sidorov, D.N.; Kurbatsky, V.G.; Panasetsky, D.A.; Zhukov, A.V.; Osak, A.B. A suite of intelligent tools for early detection and prevention of blackouts in power interconnections. *Autom. Remote Control* **2018**, *79*, 1741–1755. [\[CrossRef\]](#)
- Hassan, M.H.; Kamel, S.; Selim, A.; Khurshaid, T.; Domínguez-García, J.L. A modified Rao-2 algorithm for optimal power flow incorporating renewable energy sources. *Mathematics* **2021**, *9*, 1532. [\[CrossRef\]](#)
- Hassan, M.H.; Yousri, D.; Kamel, S.; Rahmann, C. A Modified Marine Predators Algorithm for Solving Single-and Multi-Objective Combined Economic Emission Dispatch Problems. *Comput. Ind. Eng.* **2021**, *164*, 107906. [\[CrossRef\]](#)
- Murray, A.; Engelmann, A.; Hagenmeyer, V.; Faulwasser, T. Hierarchical distributed mixed-integer optimization for reactive power dispatch. *IFAC-Pap. Line* **2018**, *51*, 368–373. [\[CrossRef\]](#)
- Kien, L.C.; Hien, C.T.; Nguyen, T.T. Optimal Reactive Power Generation for Transmission Power Systems Considering Discrete Values of Capacitors and Tap Changers. *Appl. Sci.* **2021**, *11*, 5378. [\[CrossRef\]](#)
- Venkatesh, B.; Sasadivam, G.; Khan, M.A. Towards on-line optimal reactive power scheduling using ANN memory model based method. In Proceedings of the Power Engineering Society Winter Meeting, New York, NY, USA, 31 January–4 February 1999; Volume 2, pp. 844–848.
- Grudin, N. Reactive power optimization using successive quadratic programming method. *IEEE Trans. Power Syst.* **1998**, *13*, 1219–1225. [\[CrossRef\]](#)
- Da Costa, G.R.M. Modified Newton method for reactive dispatching. *Int. J. Electr. Power Energy Syst.* **2002**, *24*, 815. [\[CrossRef\]](#)
- Rezania, E.; Shahidehpour, S.M. Real power loss minimization using interior point method. *Int. J. Electr. Power Energy Syst.* **2001**, *23*, 45–56. [\[CrossRef\]](#)
- Subbaraj, P.; Rajnarayanan, P.N. Optimal reactive power dispatch using self-adaptive real coded genetic algorithm. *Electr. Power Syst.* **2009**, *79*, 374–381. [\[CrossRef\]](#)
- Rayudu, K.; Yesuratnam, G.; Jayalaxmi, A. Improving voltage stability by optimal reactive power dispatch based on genetic algorithm and linear programming technique. In Proceedings of the International Conference on IEEE: Electrical, Electronics, and Optimization Techniques (ICEEOT), Chennai, India, 3–5 March 2016; pp. 1357–1362.

16. Villa-Acevedo, W.; López-Lezama, J.; Valencia-Velásquez, J.A. A novel constraint handling approach for the optimal reactive power dispatch problem. *Energies* **2018**, *11*, 2352. [[CrossRef](#)]
17. Alam, M.S.; De, M. Optimal reactive power dispatch using hybrid loop-genetic based algorithm. In Proceedings of the 2016 National Power Systems Conference (NPSC), Bhubaneswar, India, 19–21 December 2016; pp. 1–6.
18. Wu, Q.H.; Cao, Y.J.; Wen, J.Y. Optimal reactive power dispatch using an adaptive genetic algorithm. In Proceedings of the Second International Conference on Genetic Algorithms in Engineering Systems, Glasgow, UK, 2–4 September 1997; pp. 117–122.
19. Vaduva, A.M.; Bulac, C. New evolutionary algorithm method for solving optimal reactive power dispatch problem. In Proceedings of the International Conference on IEEE on Applied and Theoretical Electricity (ICATE), Craiova, Romania, 6–8 October 2016; pp. 1–6.
20. Mehdinejad, M.; Mohammadi-Ivatloo, B.; Dadashzadeh-Bonab, R.; Zare, K. Solution of optimal reactive power dispatch of power systems using hybrid particle swarm optimization and imperialist competitive algorithms. *Int. J. Electr. Power Energy Syst.* **2016**, *83*, 104–116. [[CrossRef](#)]
21. Singh, R.P.; Mukherjee, V.; Ghoshal, S.P. Optimal reactive power dispatch by particle swarm optimization with an aging leader and challengers. *Appl. Soft Comput.* **2015**, *29*, 298–309. [[CrossRef](#)]
22. Kanatip, R.; Keerati, C. Probabilistic optimal power flow considering load and solar power uncertainties using particle swarm optimization. *GMSARN Int. J.* **2021**, *15*, 37–43.
23. Reddy, P.L.; Yesuratnam, G. PSO based optimal reactive power dispatch for voltage profile improvement. In Proceedings of the Conference (PCITC) on IEEE Power, Communication and Information Technology, Bhubaneswar, India, 15–17 October 2015; pp. 361–366.
24. Sahli, Z.; Hamouda, A.; Bekrar, A.; Trentesaux, D. Reactive power dispatch optimization with voltage profile improvement using an efficient hybrid algorithm. *Energies* **2018**, *11*, 2134. [[CrossRef](#)]
25. Kaur, D.; Lie, T.T.; Nair, N.K.; Valles, B. An optimal reactive power dispatch (ORPD) for voltage security using particle swarm optimization (PSO) in graph theory. In Proceedings of the IEEE International Conference on Sustainable Energy Technologies (ICSET), Hanoi, Vietnam, 14–16 October 2016; pp. 25–30.
26. Polprasert, J.; Ongsakul, W.; Dieu, V.N. Optimal reactive power dispatch using improved pseudo-gradient search particle swarm optimization. *Electr. Power Compon. Syst.* **2016**, *44*, 518–532. [[CrossRef](#)]
27. Mahadevan, K.; Kannan, P.S. Comprehensive learning particle swarm optimization for reactive power dispatch. *Appl. Soft Comput.* **2010**, *10*, 641–652. [[CrossRef](#)]
28. Dieu, V.N.; Nguyen, T.P.; Nguyen, K.D. Multi-objective security constrained optimal active and reactive power dispatch using hybrid particle swarm optimization and differential evolution. *GMSARN Int. J.* **2018**, *12*, 84–117.
29. El Ela, A.A.; Abido, M.A.; Spea, S.R. Differential evolution algorithm for optimal reactive power dispatch. *Electr. Power Syst. Res.* **2011**, *81*, 458–464. [[CrossRef](#)]
30. Huang, C.M.; Huang, Y.C. Combined differential evolution algorithm and ant system for optimal reactive power dispatch. *Energy Procedia* **2012**, *14*, 1238. [[CrossRef](#)]
31. Basu, M. Quasi-oppositional differential evolution for optimal reactive power dispatch. *Int. J. Electr. Power Energy Syst.* **2016**, *78*, 29. [[CrossRef](#)]
32. Li, Y.; Li, X.; Li, Z. Reactive power optimization using hybrid CAB-DE algorithm. *Electr. Power Compon. Syst.* **2017**, *45*, 980–989. [[CrossRef](#)]
33. Ghasemi, M.; Ghanbarian, M.M.; Ghavidel, S.; Rahmani, S.; Moghaddam, E.M. Modified teaching learning algorithm and double differential evolution algorithm for optimal reactive power dispatch problem: A comparative study. *Inf. Sci.* **2014**, *278*, 231–249. [[CrossRef](#)]
34. Chen, G.; Liu, L.; Zhang, Z.; Huang, S. Optimal reactive power dispatch by improved GSA-based algorithm with the novel strategies to handle constraints. *Appl. Soft Comput.* **2017**, *50*, 58–70. [[CrossRef](#)]
35. Duman, S.; Sönmez, Y.; Güvenç, U.; Yörükeren, N. Optimal reactive power dispatch using a gravitational search algorithm. *IET Gener. Transm. Distrib.* **2012**, *6*, 563–576. [[CrossRef](#)]
36. Babu, M.R.; Lakshmi, M. Gravitational search algorithm based approach for optimal reactive power dispatch. In Proceedings of the Second International Conference on IEEE on Science Technology Engineering and Management (ICONSTEM), Chennai, India, 30–31 March 2016; pp. 360–366.
37. Rajan, A.; Malakar, T. Exchange market algorithm based optimum reactive power dispatch. *Appl. Soft Comput.* **2016**, *43*, 320–336. [[CrossRef](#)]
38. Shareef, S.M.; Rao, R.S. Optimal reactive power dispatch under unbalanced conditions using hybrid swarm intelligence. *Comput. Electr. Eng.* **2018**, *69*, 183–193. [[CrossRef](#)]
39. Mouassa, S.; Bouktir, T.; Salhi, A. Ant lion optimizer for solving optimal reactive power dispatch problem in power systems. *Eng. Sci. Technol. Int. J.* **2017**, *3*, 885–895. [[CrossRef](#)]
40. Mei, R.N.S.; Sulaiman, M.H.; Mustafa, Z.; Daniyal, H. Optimal reactive power dispatch solution by loss minimization using moth-flame optimization technique. *Appl. Soft Comput.* **2017**, *59*, 210–222.
41. Meddeb, A.; Amor, N.; Abbes, M.; Chebbi, S. A novel approach based on crow search algorithm for solving reactive power dispatch problem. *Energies* **2018**, *11*, 3321. [[CrossRef](#)]

42. Abaci, K.; Yamaçlı, V. Optimal reactive-power dispatch using differential search algorithm. *Electr. Eng.* **2017**, *99*, 213–225. [[CrossRef](#)]
43. Nuaekaew, K.; Artrit, P.; Pholdee, N.; Bureerat, S. Optimal reactive power dispatch problem using a two-archive multi-objective grey wolf optimizer. *Exp. Syst. Appl.* **2017**, *87*, 79–89. [[CrossRef](#)]
44. Anbarasan, P.; Jayabarathi, T. Optimal reactive power dispatch problem solved by an improved colliding bodies optimization algorithm. In Proceedings of the IEEE International Conference on Environment and Electrical Engineering and IEEE Industrial and Commercial Power Systems Europe (EEEIC/I&CPS Europe), Milan, Italy, 6–9 June 2017; pp. 1–6.
45. Barakat, A.F.; El-Sehiemy, R.A.; Elsaied, M.; Osman, E. Solving reactive power dispatch problem by using JAYA optimization Algorithm. *Int. J. Eng. Res. Afr. Trans. Tech. Publ.* **2018**, *36*, 12–24. [[CrossRef](#)]
46. ben oualid Medani, K.; Sayah, S.; Bekrar, A. Whale optimization algorithm based optimal reactive power dispatch: A case study of the Algerian power system. *Electric. Power Syst. Res.* **2018**, *163*, 696–705. [[CrossRef](#)]
47. Rayudu, K.; Yesuratnam, G.; Jayalaxmi, A. Ant colony optimization algorithm based optimal reactive power dispatch to improve voltage stability. In Proceedings of the International Conference on IEEE on Circuit, Power and Computing Technologies (ICCPCT), Kollam, India, 20–21 April 2017; p. 1.
48. Khazali, A.H.; Kalantar, M.O. Optimal reactive power dispatch based on harmony search algorithm. *Int. J. Electr. Power Energy Syst.* **2011**, *33*, 684–692. [[CrossRef](#)]
49. Ghasemi, M.; Taghizadeh, M.; Ghavidel, S.; Aghaei, J.; Abbasian, A. Solving optimal reactive power dispatch problem using a novel teaching-learning-based optimization algorithm. *Eng. Appl. Artif. Intell.* **2015**, *39*, 100–108. [[CrossRef](#)]
50. Rajan, T.M. Optimal reactive power dispatch using hybrid Nelder-Mead simplex based firefly algorithm. *Int. J. Electr. Power Energy Syst.* **2015**, *66*, 9–24. [[CrossRef](#)]
51. Heidari, A.A.; Abbaspour, R.A.; Jordehi, A.R. Gaussian bare-bones water cycle algorithm for optimal reactive power dispatch in electrical power systems. *Appl. Soft Comput.* **2017**, *57*, 657–671. [[CrossRef](#)]
52. Sulaiman, M.H.; Mustafa, Z.; Mohamed, M.R.; Aliman, O. Using the gray wolf optimizer for solving optimal reactive power dispatch problem. *Appl. Soft Comput.* **2015**, *32*, 286–292. [[CrossRef](#)]
53. Sulaiman, M.H.; Mustafa, Z. Cuckoo Search Algorithm as an optimizer for Optimal Reactive Power Dispatch problems. In Proceedings of the 3rd International Conference on IEEE on Control, Automation and Robotics, Nagoya, Japan, 24–26 April 2017; pp. 735–739.
54. Mukherjee, V.M. Solution of optimal reactive power dispatch by chaotic krill herd algorithm. *IET Gener. Transm. Distrib.* **2015**, *9*, 2351–2362. [[CrossRef](#)]
55. Rayudu, K.; Yesuratnam, G.; Jayalaxmi, A. Artificial Bee Colony algorithm for optimal reactive power dispatch to improve voltage stability. In Proceedings of the International Conference on IEEE on Circuit, Power and Computing Technologies (ICCPCT), Nagercoil, India, 18–19 March 2016; pp. 1–7.
56. Hassan, M.H.; Kamel, S.; El-Dabah, M.A.; Khurshaid, T.; Domínguez-García, J.L. Optimal reactive power dispatch with time-varying demand and renewable energy uncertainty using Rao-3 algorithm. *IEEE Access* **2021**, *9*, 23264–23283. [[CrossRef](#)]
57. An, N.H.T.; Dieu, V.N.; Nguyen, T.T.; Kien, V.T. One rank cuckoo search algorithm for optimal reactive power dispatch. *GMSARN Int. J.* **2015**, *73*, 82.
58. Ghasemi, M.; Davoudkhani, I.F.; Akbari, E.; Rahimnejad, A.; Ghavidel, S.; Li, L. A novel and effective optimization algorithm for global optimization and its engineering applications: Turbulent Flow of Water-based Optimization (TFWO). *Eng. Appl. Artif. Intell.* **2020**, *92*, 103666. [[CrossRef](#)]
59. Abdelminaam, D.S.; Said, M.; Houssein, E.H. Turbulent flow of water-based optimization using new objective function for parameter extraction of six photovoltaic models. *IEEE Access* **2021**, *9*, 35382–35398. [[CrossRef](#)]
60. Said, M.; Shaheen, A.M.; Ginidi, A.R.; El-Sehiemy, R.A.; Mahmoud, K.; Lehtonen, M.; Darwish, M.M. Estimating Parameters of Photovoltaic Models Using Accurate Turbulent Flow of Water Optimizer. *Processes* **2021**, *9*, 627. [[CrossRef](#)]
61. Nasri, S.; Nowdeh, S.A.; Davoudkhani, I.F.; Moghaddam, M.J.H.; Kalam, A.; Shahrokhi, S.; Zand, M. Maximum Power Point Tracking of Photovoltaic Renewable Energy System Using a New Method Based on Turbulent Flow of Water-Based Optimization (TFWO) Under Partial Shading Conditions. In *Fundamentals and Innovations in Solar Energy*; Springer: Singapore, 2021; pp. 285–310.
62. Deb, S.; Houssein, E.H.; Said, M.; Abdelminaam, D.S. Performance of Turbulent Flow of Water Optimization on Economic Load Dispatch Problem. *IEEE Access* **2021**, 77882–77893. [[CrossRef](#)]
63. Fayek, H.H.; Abdalla, O.H. Optimal Settings of BTB-VSC in Interconnected Power System Using TFWO. In Proceedings of the 2021 IEEE 30th International Symposium on Industrial Electronics (ISIE), Kyoto, Japan, 20–23 June 2021; pp. 1–6.
64. Eid, A.; Kamel, S. Optimal Allocation of Shunt Compensators in Distribution Systems using Turbulent Flow of Waterbased Optimization Algorithm. In Proceedings of the 2020 IEEE Electric Power and Energy Conference (EPEC), Edmonton, AB, Canada, 9–10 November 2020; pp. 1–5.
65. Mallipeddi, R.; Jeyadevi, S.; Suganthan, P.N.; Baskar, S. Efficient constraint handling for optimal reactive power dispatch problems. *Swarm Evol. Comput.* **2012**, *5*, 28–36. [[CrossRef](#)]
66. Nguyen, T.T.; Vo, D.N. Improved social spider optimization algorithm for optimal reactive power dispatch problem with different objectives. *Neural Comput. Appl.* **2020**, *32*, 5919–5950. [[CrossRef](#)]
67. Emery, E.; Zawbaa, H.M. Impact of chaos functions on modern swarm optimizers. *PLoS ONE* **2016**, *11*, e0158738. [[CrossRef](#)]

68. Shaheen, M.A.; Hasanien, H.M.; Alkuhayli, A. A novel hybrid GWO-PSO optimization technique for optimal reactive power dispatch problem solution. *Ain Shams Eng. J.* **2021**, *12*, 621–630. [[CrossRef](#)]
69. Shaheen, A.M.; El-Sehiemy, R.A.; Farrag, S.M. Integrated strategies of backtracking search optimizer for solving reactive power dispatch problem. *IEEE Syst. J.* **2018**, *12*, 424–433. [[CrossRef](#)]
70. Mouassa, S.; Bouktir, T. Multi-objective ant lion optimization algorithm to solve large-scale multi-objective optimal reactive power dispatch problem. *Compel.-Int. J. Comput. Math. Electr. Electron. Eng.* **2019**, *38*, 304–324. [[CrossRef](#)]
71. Mugesanyi, S.; Qu, Z.; Rugema, F.X.; Dong, Y.; Bananeza, C.; Wang, L. Optimal Reactive Power Dispatch Using Chaotic Bat Algorithm. *IEEE Access* **2020**, *8*, 65830–65867. [[CrossRef](#)]
72. Shaw, B.; Mukherjee, V.; Ghoshal, S.P. Solution of reactive power dispatch of power systems by an opposition-based gravitational search algorithm. *Int. J. Electr. Power Energy Syst.* **2014**, *55*, 29–40. [[CrossRef](#)]
73. Li, Z.; Cao, Y.; Dai, L.V.; Yang, X.; Nguyen, T.T. Finding Solutions for Optimal Reactive Power Dispatch Problem by a Novel Improved Antlion Optimization Algorithm. *Energies* **2019**, *12*, 2968. [[CrossRef](#)]